

# Northeast Church Rock 95% Design Report

## Attachment G.1: Seismic Hazard Analysis

This page intentionally left blank

## TABLE OF CONTENTS

<b>1.0 INTRODUCTION.....</b>	<b>1-1</b>
1.1 Background and Purpose.....	1-1
1.2 Approach.....	1-1
1.3 Design Criteria .....	1-1
<b>2.0 GEOLOGIC SETTING .....</b>	<b>2-1</b>
2.1 Regional Setting.....	2-1
2.2 Site Geology .....	2-1
<b>3.0 SEISMOTECTONIC SETTING AND HISTORICAL SEISMICITY .....</b>	<b>3-1</b>
3.1 Historical Seismicity .....	3-1
3.2 Catalogs of Earthquake Data .....	3-1
3.2.1 Petersen Catalog.....	3-1
3.2.2 ComCat .....	3-1
3.2.3 Combined Catalog and Magnitude Bias Correction.....	3-2
3.2.4 Man-made Earthquakes .....	3-2
3.3 Magnitude Conversion .....	3-2
3.4 Developing Recurrence Parameters .....	3-2
3.4.1 Assessment of Catalog Completeness.....	3-3
3.4.2 Estimation of the Recurrence Parameters.....	3-3
<b>4.0 SEISMIC SOURCE CHARACTERIZATION.....</b>	<b>4-1</b>
4.1 Faults .....	4-1
4.1.1 Lineaments and Monoclines .....	4-1
4.1.2 Fault Sources .....	4-2
4.1.3 Bright Angel Fault Zone .....	4-3
4.1.4 Cebollita Mesa Fault.....	4-3
4.1.5 Concho Fault .....	4-4
4.1.6 Continental Divide Fault.....	4-4
4.1.7 County Dump Fault.....	4-4
4.1.8 Coyote Wash Fault .....	4-4
4.1.9 Embudo Fault .....	4-4
4.1.10 Faults Near Cochiti Pueblo.....	4-5
4.1.11 Gallina Fault .....	4-5
4.1.12 Hickman Fault.....	4-5
4.1.13 Hubbell Spring Fault .....	4-5
4.1.14 Intrabasin Faults on the Llano de Albuquerque .....	4-5
4.1.15 Jemez-San Ysidro Fault .....	4-6
4.1.16 Jornada Draw Fault .....	4-6
4.1.17 La Bajada Fault .....	4-6
4.1.18 La Jencia Fault .....	4-6
4.1.19 Leupp Faults.....	4-7
4.1.20 Loma Pelada Fault .....	4-7
4.1.21 Manzano Fault.....	4-7
4.1.22 McCormick Ranch Fault.....	4-7
4.1.23 Nacimiento Fault.....	4-7
4.1.24 Nambe Fault .....	4-8
4.1.25 Northern Sangre de Cristo Fault.....	4-8

4.1.26	Pajarito Fault Zone .....	4-9
4.1.27	Picuris-Pecos Fault.....	4-9
4.1.28	Pojoaque Fault Zone .....	4-9
4.1.29	San Felipe Fault Zone .....	4-9
4.1.30	Sand Hill Fault Zone .....	4-10
4.1.31	San Andres Mountains Fault .....	4-10
4.1.32	Santa Fe Fault.....	4-10
4.1.33	Socorro Canyon Fault Zone.....	4-10
4.1.34	Southern Sangre de Cristo Fault .....	4-11
4.1.35	Tijeras-Cañoncito Fault System.....	4-11
4.1.36	Unnamed Fault of Bonita Canyon.....	4-11
4.1.37	Unnamed Faults along San Mateo Mountains.....	4-11
4.1.38	Unnamed Faults near Albuquerque Volcanoes .....	4-11
4.1.39	Unnamed Faults near Star Heights .....	4-12
4.1.40	Unnamed Faults of El Malpais Lava Field .....	4-12
4.1.41	Unnamed Faults on the Llano de Manzano .....	4-12
4.1.42	Vernon Fault Zone.....	4-12
4.1.43	West Joyita Fault Zone.....	4-13
4.1.44	Zia Fault.....	4-13
4.2	Colorado Plateau Areal Source.....	4-13
4.3	Shear Wave Velocity.....	4-14
<b>5.0</b>	<b>GROUND MOTION PREDICTION EQUATIONS .....</b>	<b>5-1</b>
<b>6.0</b>	<b>PROBABILISTIC SEISMIC HAZARD ANALYSIS .....</b>	<b>6-1</b>
6.1	PSHA Code and Methods.....	6-1
6.2	PSHA Inputs .....	6-1
6.2.1	Areal Source Zones.....	6-1
6.2.2	Fault Sources .....	6-1
6.3	Probabilistic Seismic Hazard Analysis Results .....	6-2
<b>7.0</b>	<b>DETERMINISTIC SEISMIC HAZARD ANALYSIS .....</b>	<b>7-1</b>
7.1	Deterministic Inputs.....	7-1
7.2	Deterministic Seismic Hazard Analysis Results.....	7-1
<b>8.0</b>	<b>RESULTS AND COMPARISON WITH PREVIOUS STUDIES.....</b>	<b>8-1</b>
<b>9.0</b>	<b>REFERENCES .....</b>	<b>9-1</b>

## LIST OF TABLES

Table 3-1:	Time Periods for Complete Event Reporting
Table 3-2:	Colorado Plateau – Magnitude Bins and Cumulative N* Values
Table 4-1:	Faults Included in Analysis
Table 4-2:	PSHA Input Parameters
Table 5-1:	GMPEs used in the PSHA
Table 6-1:	PSHA Input Parameters
Table 6-2:	PSHA Results
Table 7-1:	Deterministic Inputs and GMPEs

Table 7-2: Deterministic PGA Values

## LIST OF FIGURES

Figure 1-1: Regional Seismicity within the Study Area

Figure 2-1: Regional Faults

Figure 3-1: Seismicity of the Colorado Plateau

Figure 3-2: Catalog Completeness Plots

Figure 4-1: Gutenberg-Richter Relationship, Colorado Plateau

Figure 6-1: Peak Ground Acceleration Seismic Source Contribution for  $V_{S30}=275\text{m/s}$

Figure 6-2: Uniform Hazard Spectra Comparison of  $V_{S30}$

Figure 6-3: Deaggregation of PGA 10,000-Year Return Period for  $V_{S30}=275\text{m/s}$

Figure 6-4: Deaggregation of PGA 10,000-Year Return Period for  $V_{S30}=420\text{m/s}$

Figure 6-5: Deaggregation of PGA 10,000-Year Return Period for  $V_{S30}=566\text{m/s}$

Figure 7-1: Deterministic Response Spectra – Median and 84<sup>th</sup> Percentile for  $V_{S30}=275\text{m/s}$

Figure 8-1: Comparison of Deterministic Response Spectra and Uniform Hazard Spectra – for  $V_{S30}=275\text{m/s}$

## LIST OF ACRONYMS / ABBREVIATIONS

ANSS	Advanced National Seismic System
CEUS	Central and Eastern United States
CFR	Code of Federal Regulations
CP	Colorado Plateau
CPT	Cone Penetration Testing
DSHA	Deterministic Seismic Hazard Analysis
ft/s	feet per second
GMPE	Ground Motion Prediction Equation
ka	kilo-annum
km	kilometer
k.y.	thousand years
LLNL	Lawrence Livermore National Lab
m/s	meters per second
mm/yr	millimeters per year
m.y.	million years
Mill Site	Northeast Church Rock Mill Site
NEIC	USGS National Earthquake Information Center
NGA	Next Generation of Attenuation
NRC	US Nuclear Regulatory Agency
NSHMP	National Seismic Hazard Mapping Program
PDE	Preliminary Determination of Epicenters
PGA	Peak Ground Acceleration
PSHA	Probabilistic Seismic Hazard Analysis
SHA	Seismic Hazard Assessment
UHS	Uniform Hazard Spectra
USEPA	US Environmental Protection Agency
USGS	US Geological Survey
WUS	Western United States

## 1.0 INTRODUCTION

This report presents results of a site-specific probabilistic seismic hazard analysis (PSHA) and deterministic seismic hazard analysis (DSHA) to develop site-wide seismic design criteria at the Church Rock Mill Site (Mill Site). The Mill Site is approximately 16 miles (26 km) northeast of Gallup, New Mexico at approximately 35.65° N latitude and 108.50° W longitude.

The probabilistic seismic hazard analysis is based on a seismotectonic model and source characterization of the Mill Site and surrounding area. The study evaluated a 124-mile (200-km) radius surrounding the Mill Site. For purposes of this report, this area is termed the “study area” (Figure 1-1).

The seismotectonic model identified two general seismic sources in the study area: 1) seismicity of the Colorado Plateau (CP), and 2) crustal faults. Each source zone was characterized to establish input parameters for the seismic hazard analyses. The PSHA was performed using HAZ43 (2014) software developed by Dr. Norman Abrahamson. Long-term design recommendations were developed based on the results from this PSHA and previous seismic investigations at the site.

### 1.1 Background and Purpose

The seismic hazard assessment (SHA) was performed to estimate the seismic hazard at the project site within a probabilistic and deterministic framework by characterizing potential seismic sources. This analysis assessed the site-specific seismic hazard using Ground Motion Prediction Equations (GMPEs) to estimate seismically-induced ground motions at the Mill Site. Seismic hazard analyses were previously conducted by Lawrence Livermore National Lab (LLNL) in 1994 for the design of the uranium mill and the tailings site (NRC 1997). ~~This deterministic analysis resulted in a~~ peak ground acceleration (PGA) of 0.196 g for a magnitude of 6.25 ~~was selected by NRC (1997), based on the presence of two lineaments named the Pipeline Canyon and Wingate regional results provided by LLNL (1994) and adjusting the results for the Church Rock site.~~ [Section 8.0 provides additional details of previous seismotectonic studies performed for the project site.](#)

### 1.2 Approach

The site-specific evaluation presented herein used data from faults and earthquakes occurring within a 124-mile (200-km) radius of the Mill Site to develop seismic source characterization for the seismic hazard analyses. Stantec compiled an earthquake catalog of historical seismicity and information on specific faults to develop the seismic source models for the two seismic sources described above. The PSHA considered the defined seismic sources with the goal of identifying the major contributor(s) to the site-wide seismic hazard. Stantec performed a DSHA to evaluate ground motions associated with crustal faults likely to contribute to the site-wide seismic hazard.

### 1.3 Design Criteria

US Environmental Protection Agency (USEPA) (40 CFR 192) and the US Nuclear Regulatory Commission (NRC) (10 CFR Appendix A to Part 100 A) (NRC, 2013) guidance requires the design life for the reclaimed facility to be 1,000 years to the extent reasonably achievable, and at least 200 years. An event with a 10,000-year return period has a 2 percent probability of exceedance during a 200-year period and less than a 10 percent probability of exceedance in a 1,000-year period. Therefore, the PGA calculated using a 10,000-year return period is conservative, but appropriate for the (long-term) seismic design criteria for the Mill Site.

The PGA calculated in this PSHA will be used to evaluate long-term liquefaction potential and slope stability of the repository.

## 2.0 GEOLOGIC SETTING

### 2.1 Regional Setting

The Mill Site is located within the CP physiographic province in northwestern New Mexico. The CP is a broad, roughly circular region of relative structural stability. The contemporary seismicity of the CP was investigated by Wong and Humphrey (1989), based on seismic monitoring. Their study characterized the seismicity of the plateau as small to moderate magnitude with a low to moderate rate of widely distributed earthquakes with hypocentral depths of 9 to 12 miles (15 to 20 km). The area is characterized by generally northwest-striking normal faulting.

A 124-mile (200-km) radius surrounding the Mill Site almost all falls within the CP. However, directly to the east of the Mill Site is the Rio Grande Rift. The Rio Grande Rift system extends from southern New Mexico almost to the Colorado border with Wyoming. The rift system developed under compressional forces during the Laramide orogeny. Regional fluvial erosion and deposition, and local regional extension, modified the region such that it now consists of a series of grabens, or fault-bound down-dropped tectonic basins. Additional information on the area's geology and geomorphic features are presented in a Geohydrologic Report (Canonie, 1987), the Approved Reclamation Plan (Canonie, 1991), and Appendix I of the 95% Design Report.

### 2.2 Site Geology

A [1987](#) Geohydrologic Report (~~by Canonie Environmental, 1987~~) presents the geologic setting at the Mill Site. The Mill Site is situated on alluvial valley fill, sandstones, and shales of Cretaceous age. The stratigraphic units identified in the Mill Site area in descending order are:

- Alluvium
- Dilco Coal Member of the Crevasse canyon Formation
- Upper Gallup Sandstone, divided into:
  - Zone 3, upper sandstone
  - Zone 2, shale and coal
  - Zone 1, lower sandstone
- Upper D - Cross Tongue Member of the Mancos Shale

The alluvium and the Upper Gallup Sandstone zones are in direct contact with the existing tailings.



## 3.0 SEISMOTECTONIC SETTING AND HISTORICAL SEISMICITY

### 3.1 Historical Seismicity

The seismic hazard assessment for the Mill Site includes a review of historical earthquakes within the study area. The historical earthquake record for the study area contains earthquakes from 1887 through 2016 and provides a general overview of the seismicity of the study area. The historical seismic events were compiled from two sources: the Petersen Catalog (Petersen et al., 2014), which was used to compile earthquakes in the project region from the beginning of the catalog (1887 in the project region) to 2012; and the Advanced National Seismic System (ANSS) Comprehensive Catalog (ComCat), which was used to compile events in the region after 2012. The use of the catalogs is discussed further in Section 3.2.

Seismicity [events with moment magnitude ( $M_w$ ) greater than or equal to 2.5 ( $M_w \geq 2.5$ )] within the study area is shown in Figure 1-1. Due to diffuse events occurring within a 124-mile (200-km) radius of the Mill Site, the study area with respect to seismicity was expanded to include the entire CP as shown in Figure 3-1. The earliest recorded event included in the catalog occurred in 1887. The largest event in the catalog is a  $M_w$  6.5. Events described in this report are given in moment magnitude unless specified otherwise.

Two earthquakes were recorded within 50 km of the Mill Site: a January 5, 1976  $m_b$  5.0 earthquake approximately 27 km northeast of the site, and a March 5, 1977  $m_b$  4.6 earthquake approximately 35 km northeast of the site. These two earthquakes, collectively called the Crownpoint earthquakes due to their proximity to the town of Crownpoint in northwestern New Mexico, were the focus of a study performed by Wong et al. (1984). Wong et al. (1984) noted that these two earthquakes were unusually deep with focal depths of 41 and 44 km. Typical focal depths for earthquakes in this region are less than 20 km, and the majority of earthquakes in the region have focal depths less than 15 km (Sanford et al. 1981, Wong et al. 1984). The study concluded that due to the focal depths of the Crownpoint earthquakes, the source is likely near the Moho and are likely not associated with a geologic structure expressed at the surface. Based on this conclusion, the two earthquakes were assumed part of the background seismicity in the region, rather than associated with a fault source. As such, the Crownpoint earthquakes were included in the earthquake catalog used to develop recurrence parameters for the background seismic source. The following paragraphs summarize development of the earthquake catalog used for the SHA.

### 3.2 Catalogs of Earthquake Data

#### 3.2.1 Petersen Catalog

Stantec used catalogs from the US Geological Survey (USGS) National Seismic Hazard Mapping Program (NSHMP) for the Western United States (WUS) and Central and Eastern United States (CEUS) (Petersen et al., 2014) to compile information regarding historical earthquakes within the CP and 124 miles (200 km) of the Mill Site. Petersen et al. (2014) compiled the catalogs for the WUS and CEUS by reviewing and combining other available catalogs. Petersen et al. (2014) used their interpretation of catalog reliability to eliminate duplicate records when earthquakes were listed in more than one catalog. Since attenuation relations, completeness, and magnitude conversion rules vary regionally, Petersen et al. (2014) built two catalogs generally following the approach used by the CEUS-SSCn (NRC et al., 2012): a catalog for WUS and a catalog for the CEUS. Petersen et al. (2014) converted both catalogs to  $M_w$  from the original magnitude recorded.

Within the study area, the Petersen et al. (2014) database includes historical seismic events from 1887 through 2012 for the WUS and events from 1967 through 2012 for the CEUS. Both catalogs contain events with  $M_w \geq 2.5$ . AutoCAD software was used to delineate the CP physiographic province and identify only those events within this province. Further steps taken to develop the final catalog are discussed below. The catalog includes 412 events from the Petersen et al. (2014) database.

#### 3.2.2 ComCat

Earthquake information from the WUS and CEUS catalogs was supplemented by a search of the ANSS ComCat, also maintained by the USGS. The ComCat was used to obtain additional earthquake information from January 1, 2013 through

March 8, 2016. The ComCat contains data from networks that contribute to the ANSS database as well as historical data from the USGS National Earthquake Information Center's (NEIC) Preliminary Determination of Epicenters (PDE) catalog (<http://earthquake.usgs.gov/earthquakes/eqarchives/epic/>). The Search Earthquake Archives tool available on the USGS website (<http://earthquake.usgs.gov/earthquakes/search/>) was used to delineate a 124-mile (200-km) radius around the Mill Site to identify only those events within the seismic study area. The final catalog includes one ComCat event.

### 3.2.3 Combined Catalog and Magnitude Bias Correction

The ComCat and Petersen catalogs were combined to create a final declustered catalog for the SHA. The Petersen catalog reports magnitude as expected moment magnitude  $E[M_w]$  (Petersen et al., 2014). The conversion of the magnitude to  $E[M_w]$  for the one event from the ComCat was completed following the guidance presented in CEUS-SSCn (NRC et al., 2012). This approach is identical to that used in the development of the Petersen catalog.

The catalog includes expected magnitude  $E[M_w]$ , magnitude uncertainty, and a counting factor termed  $N^*$  (or N-star) for each event. The counting factor  $N^*$  was used to compute unbiased earthquake rates following guidance presented in CEUS-SSCn (NRC et al., 2012). Earthquake recurrence parameters were computed using the maximum likelihood approach by using the  $N^*$  factor instead of the observed counts. This approach was used for the CEUS-SSCn, which had variable levels of catalog completeness as a function of magnitude (NRC et al., 2012).

### 3.2.4 Man-made Earthquakes

Since December 2013, five mining explosions occurred within the 124-mile (200 km) radius of the Mill Site. These explosions were recorded as having magnitudes greater than 2.5 but less than 3.0. These events were not included in the catalog. It should be noted that the Petersen catalog also does not include man-made events.

Previous editions of the USGS Seismic Hazard Maps did not include earthquakes attributed to human activity. However, recent increases in man-made seismicity have prompted a change in the way these induced earthquakes are handled. The USGS released a one-year seismic hazard forecast for the Central and Eastern United States from induced and natural earthquakes (Peterson, 2016). Seventeen areas of potentially induced seismicity were considered.

The Church Rock Project Site is located more than 200 km from the nearest induced seismicity site, Raton Basin (Colorado-New Mexico) Induced Seismicity. Seismicity located at this distance would not have a significant impact on the PGA at the Mill Site.

## 3.3 Magnitude Conversion

The events included in the Petersen catalog were provided in  $M_w$ ; therefore, it was only necessary to convert the single event from the ComCat to  $M_w$ . This conversion was completed by following the approach used to compile the Petersen catalog and guidance provided in CEUS-SSCn (NRC et al., 2012).

The earthquake catalog used in recurrence calculations for this PSHA includes the combined Petersen et al. (2014) catalog and the single event from the ComCat. The final catalog includes 413 earthquakes. These earthquakes are shown on Figure 3-1.

Earthquakes included in the final catalog for the computation of recurrence parameters generally have small magnitudes, with over 99 percent of the earthquakes having a  $M_w < 5.0$  (Figure 3-1).

## 3.4 Developing Recurrence Parameters

Recurrence parameters are required to characterize seismic activity in the study area to estimate probabilistic ground motions for the Mill Site. With the exception of about 30 km on the eastern-most side of the radius, the majority of the 124-mile (200-km) radius falls within the CP physiographic province. This includes one event in the Southern Rocky Mountain physiographic province and 13 events in the Basin and Range physiographic province. The event in the Southern Rocky Mountain province is

a magnitude 2.8 and is approximately 120 miles from the Mill Site. This event was not included in the analysis. The 13 events in the Basin and Range physiographic province are within 10 km of existing faults and the faults are located at such a distance (greater than 93 miles, or 150 km) that contribution to the seismic hazard would be minimal. Only one areal source zone was delineated, the CP, as discussed in Section 4.2. The entire CP physiographic province was used to develop the recurrence parameters.

### 3.4.1 Assessment of Catalog Completeness

An assessment of the completeness of the earthquake catalog was necessary to estimate a recurrence rate for earthquakes. One way to test completeness is to plot the rate of the earthquakes (number of events greater than a specified magnitude divided by the time period) as a function of time, starting at present time and moving back towards the beginning of the catalog. If the rate of earthquakes is represented by a stationary Poisson process (the rate  $-\lambda_m$  does not change with time) for the study area, which is the typical assumption, then the rate of earthquakes should remain constant for the portions of the catalog that have complete reporting.

The evaluation was performed using the Stepp (1972) method, which includes generating completeness plots to visually inspect the rate of events over the years. Due to the diffuse seismicity within 124-mile (200-km) of the study area, the catalog was expanded to include the entire CP physiographic province. Based on this evaluation, the catalog is considered complete for the date and magnitude ranges shown in Table 3-1. The catalog completeness plots developed for this study are shown in Figure 3-2.

### 3.4.2 Estimation of the Recurrence Parameters

After completeness intervals for each magnitude range were developed, the recurrence parameters were computed. This frequency is commonly characterized using the Gutenberg-Richter relationship, which is linear when the magnitude is plotted against the frequency of events on a semi-logarithmic scale. The magnitude-frequency relation expressed in its cumulative form is:

$$\log N(M) = a - bM$$

where M is the magnitude and N is the cumulative frequency of earthquakes greater than magnitude M. The calculation of cumulative frequency of earthquakes used the N\* value (a counting factor used to compute unbiased rates) instead of observed counts. Recurrence relationships were then estimated using the maximum likelihood procedure developed by Weichert (1980). The maximum likelihood line is characterized by the slope of the line, or b-value, and the log N value at a magnitude of zero (a-value). For this study, a minimum magnitude of 3.0 was used to develop the recurrence parameters. The inputs used to calculate the recurrence parameters are summarized in Table 3-2. Recurrence parameters (a- and b-values) were developed for each seismic source zone, as discussed in Section 4.2.

## 4.0 SEISMIC SOURCE CHARACTERIZATION

The seismic source model includes crustal fault sources and the seismicity of the CP. These sources are described below.

### 4.1 Faults

A “capable fault” is defined by the NRC in 10 CFR Appendix A to Part 100, *Seismic and Geologic Siting Criteria for Nuclear Power Plants*, as a fault that has exhibited one or more of the following characteristics:

1. Movement at or near the ground surface at least once within the past 35,000 years or movement of a recurring nature within the past 500,000 years.
2. Macro-seismicity (magnitude 3.5 or greater) instrumentally determined with records of sufficient precision to demonstrate a direct relationship with the fault.
3. A structural relationship to a capable fault according to characteristics (1) or (2) above such that movement on one could be reasonably expected to be accompanied by movement on the other.

The NRC in 10 CFR Appendix A to Part 100 also indicates the minimum fault length to be considered in evaluating seismicity at a site. The minimum fault lengths with respect to distance from the site are as follows:

Distance from Site (mi)	Minimum Length of Fault to be Considered (mi)
0-20	1
20-50	5
50-100	10
100-150	20
150-200	40

#### 4.1.1 Lineaments and Monoclines

Canonie (1987) listed three local structural features near the Mill Site, noting that these local structural features are related to the regional structural features in the area including the Zuni and Defiance Uplifts and the San Juan Basin. The three local features are:

- Pipeline Canyon Lineament
- Fort Wingate Lineament
- Pinedale Monocline

The Pipeline Canyon Lineament was characterized in the Canonie (1987) report as being approximately along the axis of the Pipeline Canyon trending east-northeast in the valley. The location of the lineament was based on interpretation of aerial photos and small changes in the orientation of bedding across this feature (Canonie, 1987). No vertical or horizontal displacement was identified along the lineament at surface exposures.

The Fort Wingate Lineament was characterized in the Canonie (1987) report as being along the eastern edge of the Pipeline Canyon and trends to the north-northeast. The Fort Wingate Lineament is also mapped as a monoclinial hinge zone (Canonie, 1987).

The Pipeline Canyon and Fort Wingate Lineaments were not included in the seismic hazard analysis for several reasons. Primarily, the 1:24,000 scale geologic maps (USGS GQ-1592 and USGS GQ 1583) for the area surrounding the site does not

include these features, nor are they within the USGS Fault and Fold Database, which is a regional compilation of Quaternary active faults across the United States. Both of the geologic maps (USGS GQ-1592 and USGS GQ 1583), include structural contours that represent the base of the buried Upper Cretaceous Dakota Sandstone unit. Although the scale of the contours is general with 100 ft contours, there is no clear indication that faults are in the valley or to the east of it, which should deflect or offset the contours if there was active faulting for either or both of the mapped lineaments.

In mapping the Pipeline Canyon Lineament, the variation in the strike and dip of the beds was identified as supporting the location of this feature. It should be noted that on the geologic maps, the strike and dip data do indicate slight variance in the orientation of the beds, which is typical of minor undulations documented in the orientation of the bedrock that are not necessarily indicative of faulting. The recorded strike and dips tend to have relatively minor variance overall, well within typical normal variance range and do not necessarily indicate faulting. In general, faults mapped in the region have some degree of a normal component, which is also not visible across the canyon where the lineament is mapped.

Additionally, the Canonie (1987) report summarized that large-scale faulting is not found often in the region; however, small-scale joints and fractures, especially those related to the monoclines have been identified. Profiles included in the Canonie (1987) report that were drawn across the valley based on results of on-site drilling also do not indicate notable vertical offset across the buried bedrock units, which are generally flat-lying with some minor folding identified locally. One profile [D-D' in the Canonie (1987) report] interprets a small amount of offset for one of the units. However, the amount of offset is minor and is in between datapoints at a location where an alternative interpretation would indicate minor flattening of the unit in that location rather than an offset.

The combination of the above interpretation of the available data supports a general lack of evidence for the Pipeline Canyon and Fort Wingate Lineament features to represent active faults in this region. The overall lack of geomorphology, as well as lack of offset older bedrock, is supported by fact that these features are not included on published USGS geologic and structural maps.

The Pinedale monocline is mapped following a sinuous west-northwest trend, with up to a 20 degree dip of the beds measured on the exposed bare rock slope of the Two Wells Sandstone. The monoclinical folds in the region are described as forming the boundaries of the larger uplifts and basins (Canonie, 1987). A monocline is defined as a 'steplike bend in one direction in otherwise horizontal or gently dipping beds' (Willis, 1929). Therefore, this structure, which is mapped approximately 5 km to the south of the site, is not considered as an active fault in the seismic hazard analysis.

#### 4.1.14.1.2 **Fault Sources**

The existence and location of faults with Quaternary displacement were primarily identified using the USGS Quaternary Fault and Fold database (USGS, 2017). Faults identified with potential Quaternary-age offset that exist within a 200-mile (320-km) radius of the Mill Site are shown in Figure 2-1.

Crustal faults identified within a 200-mile (320-km) radius of the study area that satisfied the minimum fault length criteria above were included in this seismic study. This is a conservative approach because incorporating in this study all identified faults with Quaternary displacement would include faults with movement over the past 2.6 million years, whereas the NRC only requires incorporation of capable faults, which are defined in Section 4.1.1 as a fault that has shown movement within the past 35,000 to 500,000 years. Overall, 42 Quaternary faults were considered in the seismic hazard analysis and the fault parameters are provided in Table 4-1.

The USGS separates faults with Quaternary displacement into classes. These classes are provided below, as described by USGS (2017).

- For a Class A fault, geologic evidence demonstrates the existence of a Quaternary fault of tectonic origin, whether the fault is exposed by mapping or inferred from liquefaction or other deformational features.

- For a Class B fault, geologic evidence demonstrates the existence of Quaternary deformation, but either 1) the fault might not extend deeply enough to be a potential source of significant earthquakes, or 2) the currently available geologic evidence is too strong to confidently assign the feature to Class C but not strong enough to assign it to Class A.
- For a Class C fault, geologic evidence is insufficient to demonstrate: 1) the existence of tectonic faulting, or 2) Quaternary slip or deformation associated with the feature.
- For a Class D fault, geologic evidence demonstrates that the feature is not a tectonic fault or feature; this category includes features such as joints, landslides, erosional or fluvial scarps, or other landforms resembling fault scarps but of demonstrable non-tectonic origin.

The faults with Quaternary displacement included in this analysis are either Class A or Class B.

Characteristics of individual faults, including subsurface orientation, depth, slip rate, and age were obtained where possible from the USGS Quaternary Fault and Fold Database (USGS, 2017). A comprehensive list of fault characteristics used in the PSHA are included in the following subsections and inputs used in the PSHA are summarized in Table 4-2. Published fault characteristics were used when available. Typical seismogenic depths in the Western United States range from  $20 \pm 5$  km (Bott et al., 2003). However, since there is limited information on seismogenic depths near the site, a conservative seismogenic depth of 25 km was selected for the faults considered in this analysis. The probability of activity is the probability that a fault is seismogenic. For purposes of this analysis, the majority of the faults were assigned a probability of activity of 1.0; however, Class B faults were assigned a probability of activity of 0.5. The moment magnitude ( $M_w$ ) was calculated for each fault using the Wells and Coppersmith (1994) magnitude-rupture area relationship for normal faults. This relationship is:

$$M_w = 4.07 + 0.98 * \log(A)$$

where  $M_w$  is the moment magnitude and  $A$  is the rupture area in square kilometers.

#### **4.1.24.1.3** Bright Angel Fault Zone

The Bright Angel Fault Zone is approximately 200 miles (321 km) west of the Mill Site. This fault zone comprises northeast-trending faults cutting through Paleozoic rock, with movement predominantly in the normal sense as inferred from topography and exposed features (Pearthree, 1997). Quaternary deposits are sparse in the area, with no documented displacement of Quaternary alluvium; however, some fault scarps exhibit strong geomorphic expression, indicating possible Quaternary activity within this system. Although Quaternary movement has not been conclusively demonstrated in the general area, moderate historical seismic activity has occurred. A slip rate less than 0.2 mm/yr was assumed based on the lack of evidence for Quaternary movement. Dip angles range from 76 to 87 degrees and from 45 to 80 degrees, depending on the depth of the strata in question (Pearthree, 1997). Steeper dip angles were measured in Paleozoic strata, whereas shallower angles were measured for Precambrian rock strata located at greater depths within the Grand Canyon. A maximum magnitude of  $M_w$  7.3 was calculated using the Wells and Coppersmith (1994) magnitude-rupture area relationship using a maximum rupture length of 74 km.

#### **4.1.34.1.4** Cebollita Mesa Fault

The Cebollita Mesa Fault is approximately 66 miles (107 km) southeast of the Mill Site. This west-dipping normal fault has apparently young movement (less than 15 ka) (Machette and Jochems, 2016c). No dating has been performed on the scarps to refine the timing, slip rate, or recurrence. However, it is suggested that the rate is less than 0.2 mm/yr based on recent offset of 1.9 to 2.0 m, resulting from strain accumulation over 15 to 120 k.y. A maximum magnitude of  $M_w$  6.3 was calculated for a fault length of 13 km using the Wells and Coppersmith (1994) magnitude-surface rupture length relationship. Dip angles were assumed to be  $50 \pm 15$  degrees based on the regional fault dip angle (Petersen et al. 2014).

#### 4.1.44.1.5 **Concho Fault**

The Concho Fault is approximately 99 miles (160 km) southwest of the Mill site. The fault zone, located on the Mogollon Slope near the southern edge of the Colorado Plateau, consists of a discontinuous system of northwestern-trending faults that displace Mesozoic bedrock and upper to lower Pliocene basalt flows (Pearthree, 1998a). Complex surface faulting is prevalent throughout the fault zone, including multiple short fault scarps. Activity along the faults likely occurred during the middle to late Quaternary, although timing of the most recent movement is less certain. A slip rate of 0.019 to 0.040 mm/yr was estimated based on 30 m of displacement over the last 0.75 to 1.6 m.y. (Pearthree, 1998a). Both oblique normal and left-lateral movement have been inferred for this fault. Based on surface displacement, a dip to the northeast was inferred and the regional dip angle of  $50 \pm 15$  degrees was assumed (Petersen et al. 2014). A maximum magnitude of  $M_w$  7.1 was calculated for a fault length of 39 km using the Wells and Coppersmith (1994) magnitude-rupture area relationship.

#### 4.1.54.1.6 **Continental Divide Fault**

The Continental Divide Fault is approximately 63 miles (101 km) south of the Mill Site. Little is known about this northeast-trending suspect fault (Class B). A normal sense of slip was reported by Machette and Jochems (2016e). This feature appears to offset the southern part of the North Plains lava field. The dip direction was inferred from the escarpment, which faces southeast. A slip rate of less than 0.2 mm/yr was estimated based on a 2 to 3 m high scarp in Quaternary age basalt (Machette and Jochems, 2016e). A maximum magnitude of  $M_w$  6.5 was calculated for a fault length of 17 km using the Wells and Coppersmith (1994) magnitude-surface rupture length relationship. The dip angle was assumed to be  $50 \pm 15$  degrees (Petersen et al. 2014).

#### 4.1.64.1.7 **County Dump Fault**

The County Dump Fault is approximately 99 miles (160 km) southeast of the Mill Site. Located in the northern part of the Albuquerque-Belen basin, this north-trending normal fault dips to the east at an angle of 75 to 85 degrees and offsets upper Santa Fe Group deposits, well-developed calcic soils of the Llano de Albuquerque, and basalt deposits near the Albuquerque Volcanoes (Haller et al., 2015b). Repeated surface faulting has resulted in a subdued fault scarp across the Llano de Albuquerque, with a recorded height of 24 m and a maximum width of 800 m. Based on thermoluminescence aging and detailed soil analyses, the most recent activity along the surface of the fault was estimated to be about 24 ka. A slip rate of 0.015 to 0.024 mm/yr was estimated based on 24 m of displacement over the last 1 to 1.6 m.y. (Haller et al., 2015b). A maximum magnitude of  $M_w$  7.0 was calculated using the Wells and Coppersmith (1994) magnitude-rupture area relationship, based on a maximum rupture length of 35 km.

#### 4.1.74.1.8 **Coyote Wash Fault**

The Coyote Wash Fault is approximately 98 miles (158 km) southwest of the Mill Site. Similar to the Concho Fault, this fault zone is located on the Mogollon Slope between the Little Colorado River and the southern margin of the Colorado Plateau, cutting through both Mesozoic bedrock and upper to lower Pliocene basalt flows. The discontinuous system of northwestern-trending faults generally dip to the southwest, with oblique normal and left-lateral movement inferred based on fault geometry, structural characteristics, and regional relations (Pearthree, 1998b). For this assessment, the regional dip angle of  $50 \pm 15$  degrees was assumed (Petersen et al. 2014). A maximum magnitude of  $M_w$  7.1 was calculated for rupture length of 42 km using the Wells and Coppersmith (1994) magnitude-rupture area relationship, based on a maximum.

#### 4.1.84.1.9 **Embudo Fault**

The Embudo Fault is approximately 145 miles (233 km) northeast of the Mill Site along the northern and western sides of the Picuris Mountains. This near-vertical fault is an important component of the Rio Grande rift, as it accommodates differential movement of the San Luis Basin to the north and the Española Basin to the south, which dip to the east and west, respectively (Kelson et al. 2015c). For this assessment, the dip angle was assumed to be 90 degrees (vertical). The main fault strand has primarily exhibited left-lateral, strike-slip movement, whereas a normal sense of slip has been documented elsewhere along the fault where the strike direction is predominantly to the northeast. Evidence of likely repeated ruptures during the late Quaternary has been observed in Quaternary deposits along the northeastern section of the fault. A slip rate of 0.10 mm/yr was reported

based on 102 m of offset in Pliocene basalt near the town of Pilar, NM over the last 1 m.y. (Kelson et al. 2015c). A maximum magnitude of  $M_w$  7.0 was calculated using the Wells and Coppersmith (1994) magnitude-rupture area relationship, based on a maximum rupture length of 40 km.

#### **4.1.94.1.10** **Faults Near Cochiti Pueblo**

The system of faults near Cochiti Pueblo is approximately 114 miles (183 km) west of the Mill Site. Numerous faults exist in this area, including the Borrego, Peralta, Camada, Sile, Domingo, and Cochiti faults. The normal faults trend to the north-northwest and form a low-relief accommodation zone between the west-dipping Española basin to the north and east-dipping Albuquerque basin to the south (Personius and Jochems, 2016j). Offset of the lower Pleistocene Bandelier Tuff has been reported, indicating movement along the faults since the early Pleistocene, with estimated slip rates of approximately 0.042 to 0.167 mm/yr based on reported 50 to 200 m offsets over 1.2 m.y. (Personius and Jochems, 2016j). The fault dips to the west (Sawyer and Minor, 2006) at angles ranging between 60 and 75 degrees. A maximum magnitude of  $M_w$  7.0 was calculated for a rupture length of 32 km using the Wells and Coppersmith (1994) magnitude-rupture area relationship.

#### **4.1.104.1.11** **Gallina Fault**

The Gallina Fault is approximately 98 miles (157 km) northeast of the Mill Site and forms the western boundary of the Gallina-Archuleta arch. This normal fault dips at a high to nearly vertical angle towards the west and east, as suggested based on the rugged topography of the area (Kelson and Jochems, 2015). Because the actual dip angles are unknown, the fault was assumed to have the following variation in dip angles: 70 degrees to the east, 90 degrees (vertical), and 70 degrees to the west. Although there is no documented evidence for Quaternary activity, diffuse contemporary microseismicity within the Gallina-Archuleta arch may be indicative of late Quaternary activity along the fault (Kelson and Jochems, 2015). Because of the lack of geological evidence for Quaternary displacement, the slip rate is assumed to be less than 0.2 mm/yr. A maximum magnitude of  $M_w$  7.0 was calculated using the Wells and Coppersmith (1994) magnitude-rupture area relationship, based on a maximum rupture length of 39 km.

#### **4.1.144.1.12** **Hickman Fault**

The Hickman Fault is approximately 81 miles (130 km) southeast of the Mill Site. This north to northeast trending fault forms an apparent scarp on unconsolidated Quaternary deposits and may control the course of Newton Draw, a north-flowing ephemeral drainage. Chamberlin et al. (1994) reported the Hickman fault as a high angle dip-slip normal fault. This normal fault dips to the west (Machette and Jochems, 2016b) and has a reported slip rate of less than 0.2 mm/yr. A maximum magnitude of  $M_w$  6.1 was calculated for a fault length of 9 km using the Wells and Coppersmith (1994) magnitude-surface rupture length relationship. The dip angles assumed in this assessment were 60, 75, and 90 degrees (vertical), given the high angle reported by Chamberlin et al. (1994).

#### **4.1.124.1.13** **Hubbell Spring Fault**

The Hubbell Spring Fault is approximately 119 miles (192 km) southeast of the Mill Site. The fault, which forms the western edge of the Hubbell bench, comprises numerous north-striking, normal faults with well-expressed scarps 4 to 30 m high in late to early Pleistocene deposits (Haller and Personius, 2015). Based on measurement of shallow exposures, the fault dips to the west at angles ranging from 48 to 85 degrees. A slip rate between 0.2 and 1.0 mm/yr was reported based on 28 to 83 m of vertical surface displacement over 80 to 130 k.y. (Haller and Personius, 2015). A maximum magnitude of  $M_w$  7.3 was calculated for a rupture length of 74 km using the Wells and Coppersmith (1994) magnitude-rupture area relationship.

#### **4.1.134.1.14** **Intrabasin Faults on the Llano de Albuquerque**

The Intrabasin Faults on the Llano de Albuquerque are approximately 98 miles (158 km) southeast of the Mill Site. These relatively short normal faults are, for the most part, completely covered by sand such that scarps are subdued and discontinuously exposed (Jochems and Personius, 2016b). However, the fault locations have been delineated based on linear scarps, aligned drainages, and ephemeral ponds evident in aerial photographs. Although Quaternary displacement is unknown for most of the faults, slip rates of approximately 0.002 to 0.015 mm/yr were estimated based on 3 to 12 m offsets of the Llano



de Albuquerque over about 0.8 to 1.8 m.y. (Jochems and Personius, 2016b). A maximum magnitude of  $M_w$  7.4 was calculated using the Wells and Coppersmith (1994) magnitude-rupture area relationship, based on a maximum rupture length of 101 km.

#### 4.1.144.1.15 Jemez-San Ysidro Fault

The Jemez-San Ysidro Fault is approximately 94 miles (152 km) east of the Mill Site. This normal fault is separated into three continuous sections: the Jemez (northern) section, the San Ysidro (central) section, and the Calabacillas (southern) section (Jochems et al., 2016; Kelson et al., 2015h; Koning et al., 2015). The Jemez section strikes to the northeast and is marked by a prominent scarp across Virgin Mesa, which lies atop 1.2 to 1.3 Ma Bandelier tuff. Short fault scarps and fault exposures in middle and late Pleistocene alluvial deposits are characteristic of the San Ysidro section, with measured offsets of 2 to 11 m. The Calabacillas section (or Calabacillas fault) is marked by broad, dissected fault scarps with heights of 10 to 30 m on the Llano de Albuquerque, as well as some exposure in upper Santa Fe Group sediments. Slip rates range from 0.009 to 0.054 mm/yr, with the greatest rates along the Calabacillas section, based on displacement between 6 m and 50 m in material ranging in age from 0.5 Ma to 1.3 Ma (Koning et al., 2015). The dip varies from near vertical along the Jemez section, to 58 to 70 degrees east along the San Ysidro section, to 60 to 90 degrees east along the Calabacillas section. For this assessment, the dip angle was assumed to range from 58 degrees east to 90 degrees (vertical). A maximum magnitude of  $M_w$  7.4 was calculated using the Wells and Coppersmith (1994) magnitude-rupture area relationship, based on a maximum rupture length of 96 km.

#### 4.1.154.1.16 Jornada Draw Fault

The Jornada Draw Fault is approximately 189 miles (304 km) southeast of the Mill Site. Activity along this normal fault has resulted in low, subtle scarps on Quaternary deposits that mark the trace of the fault. Other factors delineating the fault include the eastward termination and offset of Tertiary bedrock and tectonically induced physiography along the hanging wall side of the fault (Machette and Jochems, 2015d,e,f). Slip rates range from 0.018 to 0.1 mm/yr across the three sections of the fault, based on reported displacements between 9 to 30 m over 300-500 k.y. The fault dips to the east and northeast, with a reported dip angle of 60 degrees to the east for the northern section (Machette and Jochems, 2015d). Dip angles were not reported for the central and southern sections, therefore the range of angles assumed in this assessment were  $60 \pm 15$  degrees to the east. A maximum magnitude of  $M_w$  7.3 was calculated for a rupture length of 65 km using the Wells and Coppersmith (1994) magnitude-rupture area relationship.

#### 4.1.164.1.17 La Bajada Fault

The La Bajada Fault is approximately 122 miles (197 km) east of the Mill Site and separates the Santo Domingo basin from the Española basin while marking the eastern edge of the Rio Grande rift. Much of the normal fault's length (primarily the northern portion) is marked by a well-developed escarpment that is several hundred meters high and faces westward (Personius and Jochems, 2016a). Quaternary activity is evident based on offset upper Pliocene and lower Pleistocene volcanic rocks; however, no scarps are evident in surficial deposits, indicating a lack of activity over the past several hundred thousand years. Estimated slip rates range from 0.079 to 0.11 mm/yr based on 90 to 250 m of displacement over 1.1 to 2.7 m.y. (Personius and Jochems, 2016a). The fault dips to the west at an angle between 55 and 90 degrees. A maximum magnitude of  $M_w$  7.1 was calculated using the Wells and Coppersmith (1994) magnitude-rupture area relationship, based on a maximum rupture length of 48 km.

#### 4.1.174.1.18 La Jencia Fault

The La Jencia Fault is approximately 121 miles (195 km) southeast of the Mill Site. The northwest-striking normal fault forms the eastern boundary of the Magdalena Mountains and the Bear Mountains, and is the tectonic margin between these mountains and the La Jencia basin located just to the east (Machette and Chamberlin, 2016). Slip rates were estimated to range from 0.033 to 0.045 mm/yr based on 5 m of displacement over 110 to 150 k.y. along the northern section of the fault. Dip generally is to the east and northeast at angles between 70 and 90 degrees as measured within 3 to 4 m of the surface; dip angles may be significantly shallower at greater depths (Machette et al., 2016a). A maximum magnitude of  $M_w$  6.9 was calculated using the Wells and Coppersmith (1994) magnitude-rupture area relationship, based on a maximum rupture length of 34 km.

#### 4.1.184.1.19 Leupp Faults

The Leupp Faults are approximately 149 miles (239 km) west of the Mill Site at the eastern edge of the San Francisco volcanic field in northern Arizona. These normal faults primarily strike towards the northwest through Paleozoic and Mesozoic bedrock, middle Pleistocene basalt, and Quaternary alluvium (Pearthree, 1998d). No known scarps exist in the Quaternary alluvium, although relatively subdued scarps have been documented in the bedrock and basalt. Because no data is available to estimate a slip rate, rates less than 0.2 mm/yr have been inferred based on documented slip rates of regional Quaternary faults (Pearthree, 1998d). Dip directions of east, northeast, and southwest were reported by Pearthree (1998d), though no dip angles were specified; therefore, for this assessment, dip angles were assumed to be 50 degrees to the west, 90 degrees (vertical), and 50 degrees to the east. A maximum magnitude of  $M_w$  7.4 was calculated using the Wells and Coppersmith (1994) magnitude-rupture area relationship, based on a maximum rupture length of 32 km.

#### 4.1.194.1.20 Loma Pelada Fault

The Loma Pelada Fault is approximately 119 miles (192 km) southeast of the Mill Site and forms the western margin of the Rio Grande rift where it meets the Sierra Ladrões and northern Lemitar Mountains. Near its northern end, this normal fault offsets Quaternary alluvium, though most of the activity along the length of the fault is evident through fault scarping and offsets in the Sierra Ladrões Formation (Personius and Jochems, 2016f). A slip rate of approximately 0.1 mm/yr was estimated based on 13 m of displacement in 130 ka Pleistocene deposits. The fault dips to the east with measured angles ranging from 60 to 80 degrees. A maximum magnitude of  $M_w$  7.1 was calculated using the Wells and Coppersmith (1994) magnitude-rupture area relationship, based on a maximum rupture length of 44 km.

#### 4.1.204.1.21 Manzano Fault

The Manzano Fault is approximately 126 miles (203 km) southeast of the Mill Site along the eastern margin of the Rio Grande rift and the Albuquerque-Belen basin. The fault is buried along the majority of its length and is primarily marked by the front of the Manzano Mountains, which form a steep, west-facing escarpment (Personius and Jochems, 2016g). Slip rates were assumed to be less than 0.2 mm/yr due to the lack of documented prominent scarps, as well as no known studies of fault offset. The normal fault dips to the west, and the dip angle was assumed to be  $50 \pm 15$  degrees (Petersen et al. 2014) for the purposes of this assessment. A maximum magnitude of  $M_w$  7.3 was calculated for a rupture length of 54 km using the Wells and Coppersmith (1994) magnitude-rupture area relationship.

#### 4.1.214.1.22 McCormick Ranch Faults

The McCormick Ranch Faults are approximately 114 miles (184 km) southeast of the Mill Site in the Albuquerque basin of the Rio Grande rift. These intrabasin, normal faults trend to the north and northeast and form numerous horst and graben blocks in the area (Personius and Jochems, 2016i). Linear scarps and depressions mark the various faults, which are partially buried in eolian sand. Offsets of 5 to 20 m have been documented for upper Santa Fe Group sediments over about 1.2 m.y., resulting in slip rates from 0.004 to 0.017 mm/yr. Dip to the east and west was reported by Personius and Jochems (2016i); because no dip angles were reported, angles of 50 degrees to the east, 90 degrees (vertical), and 50 degrees to the west were assumed for this assessment. A maximum magnitude of  $M_w$   $6.5 \pm 0.3$  was calculated using the Wells and Coppersmith (1994) magnitude-rupture area relationship, based on a maximum rupture length of 13 km.

#### 4.1.224.1.23 Nacimiento Fault

The Nacimiento Fault is approximately 77 miles (124 km) southeast of the Mill Site. The Nacimiento fault is an east-dipping normal fault bordering the Nacimiento uplift, an 80 km long, 10 to 16 km wide uplift related to Laramide deformation. This fault has two sections. Woodward (1987) mapped the Nacimiento and Pajarito faults along the western margin of the Sierra Nacimiento. He noted the lack of continuity between these faults near San Miguel Canyon section boundary, about 3 km southeast of the village of San Miguel. Wong and others (1995) considered potential fault rupture scenarios that included rupture on either a northern section or a southern section and on both sections together. This analysis includes a segmented rupture on the northern or southern segment with a weight of 0.8 and an unsegmented rupture on the complete fault with a weight of 0.2. The fault has a reported slip rate of less than 0.2 mm/yr (Kelson et al., 2015e; 2015f). This slip rate on the northern segment

is supported by the assumption of 5 m of displacement that occurred in the late Pleistocene. The slip rate on the southern section was conservatively estimated by Wong et al. (1995), to range between 0.01 to 0.23 mm/yr with a preferred value of 0.02 mm/yr. These values were used in this study for the southern section with weightings of 0.2 for a slip rate of 0.01 mm/yr, 0.6 for the preferred value of 0.2 mm/yr, and 0.2 for the 0.23 mm/yr.

For the unsegmented fault rupture, a maximum magnitude of  $M_w$  7.4 was calculated for a northern segment with a fault length of 82 km using the Wells and Coppersmith (1994) magnitude-surface rupture length relationship. The dips were assumed to be 45, 65, and 90 degrees as this spanned the range given for the northern and southern segments, 45 to 90 degrees (Kelson et al., 2015e and 2015f).

#### 4.1.22.14.1.23.1 Northern Segment

A maximum magnitude of  $M_w$  6.9 was calculated for the northern segment with a fault length of 36 km using the Wells and Coppersmith (1994) magnitude-surface rupture length relationship. In this assessment, the dips were assumed to be 45, 50, and 60 degrees as the reported range was 45 to 60 degrees (Kelson et al., 2015e).

#### 4.1.22.24.1.23.2 Southern Segment

A maximum magnitude of  $M_w$  7.0 was calculated for the southern segment with a fault length of 45 km using the Wells and Coppersmith (1994) magnitude-surface rupture length relationship. The dips were assumed to be 75, 80, and 90 degrees as the reported range was 75 to 90 degrees (Kelson et al., 2015f).

#### 4.1.234.1.24 Nambe Fault

The Nambe Fault is approximately 144 miles (232 km) east of the Mill Site. This poorly-understood fault is expressed as several north-striking normal faults along the western edge of the Sangre de Cristo Mountains north of Santa Fe, NM. The fault is thought to separate Precambrian rocks of the mountains to the east from Miocene rift-fill sediments in the Española basin to the west, though the exact nature of the contact between these two materials remains unknown. Displacement of 150-ka gravels has previously been inferred from aerial photographs, although this has neither been confirmed nor precluded (Kelson, 1996). Slip rates were assigned based on regional slip rates in the Rio Grande rift, yielding a range of 0.01 to 0.23 mm/yr with a preferred value of 0.02 mm/yr (Kelson, 1996); for this assessment, the preferred value was assigned a weight of 0.6, whereas the upper and lower end of the range (0.01 and 0.23 mm/yr) were assigned weights of 0.2. The dip was reported by Kelson (1996) as being to the west and east; because no dip angles were reported, angles of 50 degrees to the west, 90 degrees (vertical), and 50 degrees to the east were assumed for this assessment. A maximum magnitude of  $M_w$  7.1 was calculated using the Wells and Coppersmith (1994) magnitude-rupture area relationship, based on a maximum rupture length of 48 km.

#### 4.1.244.1.25 Northern Sangre de Cristo Fault

The Northern Sangre de Cristo Fault is approximately 198 miles (319 km) northeast of the Mill Site. This north-northwest striking normal fault forms the boundary between the Sangre de Cristo/Culebra Range and the San Luis basin of the Rio Grande rift in southern Colorado. The fault contains four main sections (listed from north to south): the Crestone section, the Zapata section, the Blanca section, and the San Luis section. The Crestone section exhibits prominent but discontinuous west-facing scarps on late Quaternary deposits (Kirkham and Haller, 2015). These continue into the Zapata section, becoming less numerous further south along this section yet still indicative of repeated late Quaternary activity (Kirkham and Haller, 2012a). Along the Blanca section, scarps as high as 28.3 m associated with a prominent graben 2.1 km in length exist on glacial and alluvial deposits (Kirkham, 2012). Activity is also evident along the San Luis section, with escarpments as high as 35 m along the fault (Kirkham and Haller, 2012b). Age/offset information for calculating slip rates only exists for the Crestone section, though all sections fall into the low slip-rate category (i.e., less than 0.2 mm/yr). For the Crestone section, a maximum slip rate of 0.164 mm/yr was estimated based on 4.5 m of surface offset over 27.4 k.y., though the reported average slip rate is only 0.044mm/yr (Kirkham and Haller, 2015). All sections of the fault dip to the west or southwest at angles estimated to be about 60 degrees in some areas. Because the dip angle is uncertain along much of the fault, the regional fault dip angle of  $50 \pm 15$  degrees was assumed

(Petersen et al. 2014) in this assessment. A maximum magnitude of  $M_w$  7.7 was calculated using the Wells and Coppersmith (1994) magnitude-rupture area relationship, based on a maximum rupture length of 168 km.

#### **4.1-254.1.26 Pajarito Fault Zone**

The Pajarito Fault Zone is approximately 121 miles (195 km) east of the Mill Site near Los Alamos, NM. The southern portion of the normal fault, which has been extensively studied, comprises broadly distributed faults, fissures, and folds striking to the north and offsetting early Quaternary volcanic rocks, as well as younger alluvium (Haller et al., 2015a). Prominent, west-facing scarps exist along the length of the fault traces, with heights as great as 200 m. The fault system as a whole is as wide as 10 km and accommodates much of the Quaternary east-west extension of the Española basin in the area. Slip rates were estimated to range from 0.033 to 0.167 mm/yr based on 40 to 200 m of displacement of the Bandelier Tuff (1.2 Ma). Although Haller et al. (2015a) reported dip to the east for the entire fault, data fully characterizing the surface and subsurface are lacking and it is believed that the fault zone may be listric below depths of 10 km. For this assessment, the regional dip angle of  $50 \pm 15$  degrees was assumed (Petersen et al. 2014). A maximum magnitude of  $M_w$  7.2 was calculated using the Wells and Coppersmith (1994) magnitude-rupture area relationship, based on a maximum rupture length of 49 km.

#### **4.1-264.1.27 Picuris-Pecos Fault**

The Picuris-Pecos Fault, identified by USGS as a Class B fault, is approximately 148 miles (238 km) east of the Mill Site within the Sangre de Cristo Mountains of New Mexico. This north-northeast striking normal fault is well-expressed and known to have undergone displacement during Precambrian, Pennsylvanian, late Cretaceous, and possibly Neogene times; however, no evidence has been documented indicating displacement of Quaternary deposits, partly due to an overall lack of such deposits in the locally rugged terrain (Kelson and Jochems, 2016a). Previous conservative estimates of slip rates, based on analysis of both regional slip rates and the geomorphic expression of the Picuris-Pecos fault, ranged from 0.01 to 0.45 mm/yr with a preferred value of 0.05 mm/yr. For this assessment, the preferred value was given a weight of 0.6 whereas the upper and lower end of the range were assigned weights of 0.2. In general, the fault dips nearly vertically; for the purposes of this assessment, the fault was assigned dip angles of 70 degrees west, 90 degrees (vertical), and 70 degrees east. A maximum magnitude of  $M_w$  7.4 was calculated using the Wells and Coppersmith (1994) magnitude-rupture area relationship, based on a maximum rupture length of 98 km.

#### **4.1-274.1.28 Pojoaque Fault Zone**

The Pojoaque Fault Zone is approximately 137 miles (221 km) east of the Mill Site in the Española Basin. This poorly-understood fault zone comprises multiple north-striking normal faults over approximately a 5-km-wide area. The location of the fault and activity are uncertain, and little geomorphic expression is evident where faults have been traced. Possible Quaternary activity is suggested based on fault orientation and association with the Velarde graben (Kelson and Personius, 1996). Estimated slip rates based on regional slip rates in the Rio Grande rift range from 0.01 to 0.23 mm/yr, with a preferred value of 0.02 mm/yr (Kelson and Personius, 1996). The dip of the fault has been noted as down to both the east and west at a high angle, although the overall sense of displacement dips to the west. For this assessment, the fault was assumed to have dip angles of 60 degrees west, 90 degrees (vertical), and 60 degrees east. A maximum magnitude of  $M_w$  7.1 was calculated using the Wells and Coppersmith (1994) magnitude-rupture area relationship, based on a maximum rupture length of 48 km.

#### **4.1-284.1.29 San Felipe Fault Zone**

The San Felipe Fault Zone is approximately 102 miles (164 km) east of the Mill Site in the Santo Domingo basin of the Rio Grande rift. Numerous north-trending normal faults make up the two sections of this fault zone, with the western, east-dipping faults comprising the Santa Ana section, and the eastern, west-dipping faults comprising the Algodones section (Personius et al., 2016a,b). The faults form the San Felipe graben, offsetting 2.4 to 2.6 Ma volcanic basalt flows. Fault expression is greatest in the basalt flows of the San Felipe volcanic field, whereas faults located in Santa Fe Group sedimentary rocks are poorly expressed (Personius et al., 2016a,b). Estimated slip rates range from 0.035 to 0.05 mm/yr based on 90 to 120 m of displacement in the San Felipe basalt over 2.4 to 2.6 m.y. Dip angles of 64 to 74 degrees to the west were reported for the Algodones section, whereas angles of 60 to 90 degrees to the east were reported for the Santa Ana section; for this assessment,

assumed dip angles for the unsegmented fault were 60 degrees east, 90 degrees (vertical), and 64 degrees west. A maximum magnitude of  $M_w$  7.4 was calculated for a rupture length of 89 km using the Wells and Coppersmith (1994) magnitude-rupture area relationship.

#### **4.1.294.1.30 Sand Hill Fault Zone**

The Sand Hill Fault Zone is approximately 93 miles (150 km) east of the Mill Site and is one of several faults that form part of the active western boundary of the Rio Grande rift in the region. This north-trending, normal fault cuts through early Pleistocene sand and gravel of the upper Santa Fe group, with younger surficial deposits atop the fault that do not exhibit faulting. In general, there is a lack of fault scarps, and the fault strands are marked by sand dikes that are more resistant to erosion than the surrounding Santa Fe Group sediments. Based on the lack of scarps, as well as low known slip rates for other faults in the region, a general slip-rate category of less than 0.2 mm/yr was assigned to this fault (Personius and Jochems, 2016b). The fault dips to the east at angles ranging from 54 to 82 degrees as measured from surface exposures. A maximum magnitude of  $M_w$   $7.0 \pm 0.3$  was calculated using the Wells and Coppersmith (1994) magnitude-rupture area relationship based on a maximum rupture length of 36 km.

#### **4.1.304.1.31 San Andres Mountains Fault**

The San Andres Mountains Fault is approximately 193 miles (311 km) southeast of the Mill Site. This normal fault trends to the north along the eastern boundary of the San Andres Mountains where they meet the Tularosa basin. Uplift of the San Andres Mountains can be attributed to this fault, as shown by exposed Precambrian and Paleozoic rocks along the footwall of the fault (Machette and Jochems, 2015a; 2015b; 2015c). Faulting of middle to late Quaternary surficial deposits is evident via mostly continuous scarps along the fault trace, as well as some discontinuous scarps along northern portions of the fault. Estimated slip rates range from 0.002 mm/yr along the northern section of the fault to 0.21 mm/yr along the central and southern sections, based on scarps heights from 2 to 15 m in middle to late Pleistocene deposits (northern section) and Picacho alluvium (central and southern sections). The fault dips to the east; due to a lack of measured dip angles, values were assumed for this assessment based on the regional fault dip angle of  $50 \pm 15$  degrees. A maximum magnitude of  $M_w$  7.6 was calculated using the Wells and Coppersmith (1994) magnitude-rupture area relationship based on a maximum rupture length of 114 km.

#### **4.1.314.1.32 Santa Fe Fault**

The Santa Fe Fault is approximately 95 miles (153 km) southeast of the Mill Site along the western margin of the Rio Grande rift and separates the rift from the Colorado Plateau. Documented offset of upper Santa Fe Group sediments is indicative of significant activity during the Pliocene and early Pleistocene on this north-trending, normal fault. Although no surficial deposit scarps have been observed, the fault forms a bedrock escarpment along its northern half (Personius and Jochems, 2015). A low slip rate of approximately 0.008 mm/yr was estimated based on 30 m of displacement of basalt deposits over about 3.7 m.y. The fault dips to the east at an angle ranging from 45 to 80 degrees. A maximum magnitude of  $M_w$  6.9 was calculated using the Wells and Coppersmith (1994) magnitude-rupture area relationship, based on a maximum rupture length of 30 km.

#### **4.1.324.1.33 Socorro Canyon Fault Zone**

The Socorro Canyon Fault Zone is approximately 130 miles (210 km) southeast of the Mill Site. This normal fault consists of two sections, northern and southern, which define the eastern margin of the Socorro and northern Lemitar Mountains along the western edge of the Rio Grande Valley. About 208 m of displacement of a 4.0 Ma basalt is evident, although displacement during the Pliocene through Pleistocene likely is less than 300 m. Discontinuous and obscure scarps are present along parts of the northern section, including many that are mostly buried by colluvium or possible landslide debris, whereas scarps along the southern section are more continuous (Machette and Chamberlin, 2015; Machette et al., 2016b). Although little offset or age data exist for the northern section of the fault, slip rates along the southern section are estimated to range from 0.03 to 0.6 mm/yr based on movement ranging from 30 m over 1 m.y. to 0.6 m over only 100 years (estimated modern rate of deformation, possibly a result of draping). The fault dips to the east at angles ranging from 36 degrees to 90 degrees (vertical) along both sections of the fault. A maximum magnitude of  $M_w$  7.1 was calculated using the Wells and Coppersmith (1994) magnitude-rupture area relationship, based on a maximum rupture length of 49 km.

#### **4.1.334.1.34 Southern Sangre de Cristo Fault**

The Southern Sangre de Cristo Fault is approximately 169 miles (272 km) northeast of the Mill Site, forming the boundary between the Sangre de Cristo Mountains and the San Luis basin in New Mexico and between San Pedro Mesa and San Luis Valley in Colorado (Kelson et al., 2015a,b,d,g). The normal fault is subdivided into five sections (listed from north to south): the San Pedro Mesa section, the Urraca section, the Questa section, the Hondo section, and the Cañon section. Much of the length of the San Pedro Mesa section is buried by Quaternary landslide deposits, although discontinuous scarps can be seen among and between the deposits (Kelson et al., 2015a,b,d,g). Other sections of the fault contain prominent scarps on late Pleistocene and (possibly) Holocene alluvial fans originating from the Sangre de Cristo Mountains. Reported slip rates range from 0.01 to 0.23 mm/yr, although two primary ranges in vertical displacement rates have been estimated for much of the fault: a post-middle Pleistocene rate of 0.03 to 0.06 mm/yr and a post-Pliocene rate of 0.12 to 0.23 mm/yr (Kelson et al., 2015a,b,d,g; Kelson et al., 1998). The dip for fault sections is to the west at an angle of approximately 60 degrees. A maximum magnitude of  $M_w$  7.5 was calculated using the Wells and Coppersmith (1994) magnitude-rupture area relationship, based on a maximum rupture length of 99 km.

#### **4.1.344.1.35 Tijeras-Cañoncito Fault System**

The Tijeras-Cañoncito Fault System is approximately 121 miles (195 km) east of the Mill Site and forms the structural boundary separating the Española basin of the Rio Grande rift from the Great Plains tectonic province. This fault strikes to the northeast and shows evidence of left-lateral, normal movement. Displacement of Quaternary deposits has been observed in surface sediments along the Canyon section of the fault, which exhibits prominent scarps as well as juxtaposition of different rock types. Alternatively, the Galisteo section appears to have no geomorphic expression associated with late Quaternary fault movement (Kelson and Jochems, 2016b,c). Slip rates are reported to range from 0.02 to 0.72 mm/yr, with a preferred value of 0.09 mm/yr. For this assessment, the preferred value was assigned a weight of 0.6, whereas the upper and lower end of the reported range of slip rates were given weights of 0.2. Dip along this fault is nearly vertical. A maximum magnitude of  $M_w$  7.3 was calculated using the Wells and Coppersmith (1994) magnitude-rupture area relationship based on a maximum rupture length of 79 km.

#### **4.1.354.1.36 Unnamed Fault of Bonita Canyon**

The Unnamed fault of Bonita Canyon is approximately 55 miles (88 km) southeast of the Mill Site. The suspect fault of Bonita Canyon is identified as a Class B fault and there are no detailed studies of the normal fault. However, fault scarp-like features have been mapped on the early Quaternary Twin Craters and El Calderon basalt flows of El Malpais lava field. No measurement of offset across the fault has been reported. It is undetermined if the scarps are formed on an early Quaternary age landscape, and therefore this fault is assigned a slip rate less than 0.2 mm/yr (Machette and Jochems, 2016d). Because the dip direction is unknown, the input into the PSHA was varied as follows: 50 degrees to the east, 90 degrees (vertical), and 50 degrees to the west. A maximum magnitude of  $M_w$  6.1 was calculated for a fault length of 9 km using the Wells and Coppersmith (1994) magnitude-surface rupture length relationship.

#### **4.1.364.1.37 Unnamed Faults along San Mateo Mountains**

The Unnamed Faults along San Mateo Mountains are approximately 145 miles (233 km) southeast of the Mill Site. This group of normal faults strike to the north near the eastern margin of the San Mateo Mountains. Relatively small west-facing scarps are apparent along the fault and contrast the down-to-the-east slope of the piedmont surfaces through which the fault cuts (Machette and Jochems, 2016a). Slip rates were estimated to range from 0.009 to 0.011 mm/yr based on the maximum documented scarp height of 8 m formed on the Palomas Formation over approximately 700 to 900 k.y. As previously noted, dip is to the west at angles assumed to coincide with the regional fault dip angle of  $50 \pm 15$  degrees (Petersen et al. 2014). A maximum magnitude of  $M_w$  7.1 was calculated for a rupture length of 41 km using the Wells and Coppersmith (1994) magnitude-rupture area relationship.

#### **4.1.374.1.38 Unnamed Faults near Albuquerque Volcanoes**

The Unnamed Faults near Albuquerque Volcanoes are approximately 101 miles (162 km) southeast of the Mill Site in the middle of the Albuquerque-Belen basin of the Rio Grande rift. Most of these north-trending, normal faults cut through upper Santa Fe

Group sediments that lie beneath volcanic basalt flows dated to between 155 to 218 ka, although at least two faults offset the basalt as evidenced by prominent, linear scarps (Personius and Jochems, 2016d). These scarps are about 1 to 2 m in height, resulting in an estimated slip rate of 0.005 to 0.013 mm/yr based on the age of the basalt flows. Faults dip to both the east and the west; for this assessment, dip angles were assumed to be 50 degrees east, 90 degrees (vertical), and 50 degrees west. A maximum magnitude of  $M_w$  6.9 was calculated using the Wells and Coppersmith (1994) magnitude-rupture area relationship, based on a maximum rupture length of 34 km.

#### **4.1.384.1.39 Unnamed Faults near Star Heights**

The Unnamed Faults near Star Heights are approximately 101 miles (163 km) east of the Mill Site in the northern part of the Albuquerque-Belen basin. These intrabasin, normal faults strike to the north, offsetting upper Santa Fe Group sediments, the Llano de Albuquerque, and younger piedmont deposits (Personius and Jochems, 2016c). Scarps on the Llano de Albuquerque are relatively broad and 15 to 20 m in height, whereas scarps on the Piedmont deposits are relatively steep and 5 to 10 m in height. A slip-rate category of less than 0.2 mm/yr was inferred by Personius and Jochems (2016c) based on the broad scarps observed on the Llano de Albuquerque. The faults generally dip to the east at an angle of 70 degrees. A maximum magnitude of  $M_w$  6.7 was calculated using the Wells and Coppersmith (1994) magnitude-rupture area relationship based on a maximum rupture length of 18 km.

#### **4.1.394.1.40 Unnamed Faults of El Malpais Lava Field**

The Unnamed faults of El Malpais lava field are approximately 55 miles (89 km) southeast of the Mill Site. Four groups of suspect faults, which the USGS classifies as Class B, form numerous fissures and cracks in early Quaternary basalt flow of El Malpais lava field. There is some debate whether the faults are of tectonic origin. The longest feature, named La Rendija by Levish et al. (1992), is 26 km long. As with the majority of the faults in the CP, the sense of slip is normal, but the dip direction is listed as west, northwest, and east (Machette and Jochems, 2016f). Therefore, the dip direction was varied 50 degrees to the east, 90 degrees (vertical), and 50 degrees to the west. Only the longest feature was included in the PSHA, as the other features were less than 5 km long. A maximum magnitude of  $M_w$  6.7 was calculated for a fault length of 26 km using the Wells and Coppersmith (1994) magnitude-surface rupture length relationship.

#### **4.1.404.1.41 Unnamed Faults on the Llano de Manzano**

The Unnamed Faults on the Llano de Manzano are approximately 126 miles (203 km) southeast of the Mill Site. These normal faults strike to the northeast and offset the Llano de Manzano by about 5 to 10 m in multiple locations, as shown by subdued scarps that are discontinuously preserved and covered by eolian sand. Although most of the faults are intrabasin faults, the southernmost faults potentially mark the eastern margin of the Rio Grande rift (Jochems and Personius, 2016a). Slip rates were estimated to range from 0.005 to 0.02 mm/yr based on 5 to 20 m of displacement of the Llano de Manzano over approximately 1 m.y. The faults are reported to dip to both the east and west; for this assessment, dip angles were assumed to be 50 degrees to the east, 90 degrees (vertical), and 50 degrees to the west. A maximum magnitude of  $M_w$  7.2 was calculated using the Wells and Coppersmith (1994) magnitude-rupture area relationship, based on a maximum rupture length of 68 km.

#### **4.1.414.1.42 Vernon Fault Zone**

The Vernon Fault Zone is approximately 109 miles (176 km) southwest of the Mill Site on an erosion surface sloping north from the boundary of the Colorado Plateau towards the Little Colorado River. Left-lateral and normal movement through Mesozoic bedrock, Miocene volcanic rocks, and upper to lower Pleistocene basalt has been inferred for these northwest-trending faults based on fault geometry and topography, although specific amounts of displacement remain unknown (Pearthree, 1998c). Scarps are known to be somewhat subdued and of low to moderate height, although no specific scarp data has been reported. Because of a lack of reported slip rate data, the faults were assigned a slip-rate category less than 0.2 mm/yr. The faults dip to the northeast, and dip angles were assumed for this assessment based on the regional fault dip angle of  $50 \pm 15$  degrees (Petersen et al. 2014). A maximum magnitude of  $M_w$  7.3 was calculated using the Wells and Coppersmith (1994) magnitude-rupture area relationship, based on a maximum rupture length of 57 km.

#### 4.1.424.1.43 West Joyita Fault Zone

The West Joyita Fault Zone is approximately 132 miles (212 km) southeast of the Mill Site along the eastern margin of the Rio Grande rift. The zone of normal faults is poorly expressed over much of its area, except on the west flank of the northernmost Joyita Hills where upper Santa Fe Group sediments are clearly juxtaposed with Paleozoic rock (Personius and Jochems, 2016e). Although much of the fault zone is buried by middle Pleistocene and younger rocks, offset greater than 150 m has been documented in the early Pleistocene Sierra Ladrones Formation in the northern portion of the zone. A slip rate category of less than 0.2 mm/yr was assigned to these faults based on reported offset/age estimates. The fault dips generally to the west at angles ranging from 41 to 80 degrees based on dip data for the southern end of the zone. A maximum magnitude of  $M_w$  7.1 was calculated using the Wells and Coppersmith (1994) magnitude-rupture area relationship, based on a maximum rupture length of 48 km.

#### 4.1.434.1.44 Zia Fault

The Zia Fault is approximately 98 miles (157 km) east of the Mill Site. This intrabasin, normal fault trends to the north and is well exposed in the Santa Fe Group sediment of the Zia badlands. To the south, broad, dissected scarps are evident on the Llano de Albuquerque and younger surficial deposits (Personius and Haller, 2015). Slip rates ranging from 0.055 to 0.103 mm/yr were estimated based on 6.5 m of offset of Santa Fe Group sediments over 63 to 119 k.y. The faults dip to the east, and dip angles were assumed for this assessment based on the regional fault dip angle of  $50 \pm 15$  degrees (Petersen et al. 2014). A maximum magnitude of  $M_w$  7.0 was calculated using the Wells and Coppersmith (1994) magnitude-rupture area relationship, based on a maximum rupture length of 32 km.

## 4.2 Colorado Plateau Areal Source

The seismic hazard from background events unassociated with known faults was assessed by first looking at the 124-mile (200-km) radius around the Mill Site. The majority of this radius fell within the CP physiographic province (Figure 2-1). The areal source zone was then expanded to include the entire CP (Figure 3-1).

Boundaries of the areal source zone were developed based on regional geology, tectonic regime, and similar patterns of historical seismicity. The CP boundary (Figure 3-2) was based on observed seismicity and the delineation provided by Sbar (1982). Catalog seismicity within the source zone was used to estimate the Gutenberg-Richter  $a$  and  $b$  parameters. Earthquake locations within each zone are assumed to be uniformly located within the space. Parameters for defining seismicity within each source zone include the following: minimum and maximum depth, activity rate (number of events per year  $> M_{min}$ ) and  $b$ -value estimated from the historical seismicity catalog for the zone, probability of activity, and parameters for rupture length estimation based on magnitude.

The Mill Site is located within the CP, as shown on Figure 1-1. This zone exhibits relatively sparse concentrations of earthquake events. As discussed in Section 3.3, 413 events were included in the catalog between 1887 and 2016 within the CP source zone. The largest earthquake event within the CP source zone developed for this project was a  $M_w$  6.5 event that occurred on November 14, 1901, approximately 292 miles (470 km) from the Mill Site. Based on the historical seismicity, the closest event was an  $M_w$  4.7 event that occurred on January 5, 1976, approximately 16 miles (26 km) from the Mill Site.

As discussed previously, the  $a$ - and  $b$ -values for the Gutenberg-Richter recurrence relationship were estimated using the maximum likelihood method developed by Weichert (1980) and the collected seismicity for the project-specific CP source zone. The estimated  $b$ -value for the CP is 0.84 and the calculated activity rate is 0.19 earthquake events per year greater than  $M_w$  5.0. In order to include epistemic uncertainty in the recurrence parameters, the  $a$ -value was held constant while the  $b$ -value was varied  $\pm 0.05$  units. Figure 4-1 shows the fit of the recurrence relationship to the seismicity data used in the development of the  $a$  and  $b$  parameters, along with a representation of the truncated exponential recurrence relationship used in the PSHA. A maximum magnitude of 6.5 is the largest earthquake in the study area and a standard error of  $\pm 0.25$  was added for an upper estimate of  $M_w$  of 6.75. This is consistent with the maximum magnitude of  $M_w$  6.75 for the CP, as discussed by Wong and Olig (1998). The maximum depth of events specified for the CP is 15.5 miles (25 km).



### 4.3 Shear Wave Velocity

The shear wave velocity was estimated in the top 100 feet (30 meters,  $V_{s30}$ ) of the original ground surface. The tailings were not considered in estimating the shear wave velocity because this site-wide SHA was performed to estimate peak accelerations at the original ground surface. As previously mentioned, the Mill Site is situated on an alluvial valley and the subsurface profile can vary from 30 m of soil (alluvium) to 30 m of rock (Sandstone). Therefore, the shear wave velocity was estimated for both an alluvium site and a soft rock site. The following paragraphs summarize the method used to calculate and estimate a site-specific shear wave velocity for use in the seismic hazard analysis.

ConeTec measured the shear-wave velocity via cone penetration testing (CPT) in November 2013. Because the CPT was limited to soft soils, most of the measurements are within the existing tailings and alluvium, not the sandstone. RCPT-11 extended to a depth of 26 meters, with the top 9 meters within existing tailings and approximately 17 meters of alluvium. For the CPT performed as part of this investigation, location RCPT-11 encountered the maximum depth of alluvium. The shear wave velocity for this CPT location in the alluvium varied from 202 to 292 m/s. The Boore (2004) regression coefficients were used to extrapolate the velocity data in the alluvium to a depth of 30 meters. This resulted in a  $V_{s30}$  equal to 275 m/s.

No site-specific shear wave velocity measurements are available for the sandstone; therefore, published values for sandstone were used. Wills and Clahan (2006) published mean  $V_{s30}$  values for a variety of California geological units. The shear wave velocity was measured at six sites underlain by Cretaceous sandstone by Wills and Clahan (2006). The authors provide a mean  $V_{s30}$  of 566 m/s for this material. The sandstone underlying the site is Cretaceous, and therefore, a  $V_{s30}$  value of 566 m/s was used in this analysis.

Site-specific  $V_{s30}$  values used in the seismic hazard analyses are as follows: 275 m/s for the alluvium, 566 m/s for the sandstone, and 420 m/s (the average of the alluvium and sandstone  $V_{s30}$  values). The three  $V_{s30}$  values were selected to represent the range of alluvium thickness within the foundation, which varied between approximately 0 and 100 feet thick.

## 5.0 GROUND MOTION PREDICTION EQUATIONS

GMPEs are applied to earthquakes to estimate ground motion at the Mill Site. GMPEs are mathematical expressions that define how seismic waves propagate from the source to the site. Several factors combine to decreased amplitude or intensity as the wave travels to the site, including refraction, reflection, diffraction, geometric spreading, and absorption.

GMPEs estimate ground motion as a function of magnitude, distance, and site conditions (e.g. soil, rock, or  $V_{s30}$ ). The relationships are derived by fitting equations to data obtained by strong-motion instruments for a specific region.

Current Next Generation of Attenuation (NGA) West 2 relationships were used for the crustal faults and the areal source zone: Abrahamson, et al. (2014), Boore, et al. (2014), Campbell and Bozorgnia (2014), and Chiou and Youngs (2014). Idriss (2014) was not used due to limitations on the maximum distance and minimum  $V_{s30}$  value. The maximum applicable distance for Idriss (2014) is limited to 93 miles (150 km) and the  $V_{s30}$  value for the GMPE is limited to a minimum of 450 m/s.

The GMPEs were equally weighted. It should be noted that the GMPEs implemented in this study were developed using the most current information, and these models have been shown to be applicable worldwide. Table 5-1 lists the relationships and the associated weights.

## 6.0 PROBABILISTIC SEISMIC HAZARD ANALYSIS

The following sections describe the PSHA methods, inputs for analysis, and results.

### 6.1 PSHA Code and Methods

The methods for PSHA was developed by Cornell (1968), and was used to provide a framework in which uncertainties in size, location, and rate of recurrence of earthquakes can be considered to provide a probabilistic understanding of seismic hazard.

A PSHA can be described as a procedure of four steps (Kramer 1996):

- Identification and characterization of earthquake sources, along with the assignment of a probability distribution to each source zone
- Characterization of earthquake recurrence
- Estimation of ground motion produced at the site by earthquakes of any possible size occurring at any possible point in each source zone
- Calculation of the probability that the ground motion parameter will be exceeded during a particular time period given uncertainties in earthquake location, earthquake size and ground motion parameters

Calculations for this report were performed using the computer code HAZ43b, developed by Dr. Norman Abrahamson. Earlier versions of this code were verified under the PEER PSHA Code Verification Workshop (Thomas et al., 2010).

### 6.2 PSHA Inputs

The PSHA considered a combination of areal and fault sources. Exponential relationships were developed to characterize the seismicity of the areal source zone. Historical seismicity was used to characterize activity based on Gutenberg-Richter relationships within the CP seismic zone that are shown in Figure 3-1. The areal source is described in Section 4.2 and the GMPEs considered are explained in Section 5.0.

Additional input parameters [depth to (1.0 km/s) ( $Z_{1.0}$ ) and depth to (2.5 km/s) ( $Z_{2.5}$ )] were estimated from the input  $V_{s30}$  value. Each of these values are summarized in Table 6-1.

#### 6.2.1 Areal Source Zones

Characteristics of the CP areal source zone included in this analysis are described in Section 4.2. The earthquake recurrence for the areal source zone was based on the rate of historical seismicity within this zone and does not include Gaussian smoothing. The estimation of the recurrence parameters for the areal source zone was presented in Section 4.2. Although recurrence parameters were developed considering events with magnitudes as low as  $M_w$  3.0, a minimum magnitude of  $M_w$  5.0 was used in the probabilistic analysis, as events with magnitudes less than  $M_w$  5.0 are unlikely to generate a significant hazard at the Mill Site. The maximum magnitude assigned to the areal source zone was  $M_w$  6.75.

#### 6.2.2 Fault Sources

Quaternary faults that fell within a 200-mile (322-km) radius were included in the analysis. In general, fault sources beyond 200-miles were judged to not contribute to the seismic hazard, due to their site-to-source distance and likely dominant contribution of the areal background source. The mapped fault lineation (USGS, 2017) was simplified in the analysis by tracing the mapped lineation and redrawing the faults as they appear in Figure 2-1. To account for uncertainty in estimating the maximum magnitude of these faults, the maximum magnitude in the PSHA were varied by  $\pm 0.3$  magnitude units, with the central values (calculated maximum magnitude value) weighted with 0.6, and the upper and lower values weighted with 0.2.

Fault recurrence were modeled as both characteristic and maximum magnitude. Characteristic events were assigned a probability of 0.7 and the maximum magnitude model was weighted 0.3. The weighting was set to balance out the two different models.

Additional information on the fault parameters for the PSHA, including dip, slip rate, depth, type of fault, and weighting, is included in Table 4-2.

### 6.3 Probabilistic Seismic Hazard Analysis Results

Ground motions at the Mill Site were calculated for the average horizontal component of motion in terms of PGA. In order to bracket the PGA and account for uncertainty in the site-specific  $V_{s30}$ , the PGA was calculated for the range of  $V_{s30}$  values presented in Section 4.3.3. The results are summarized in Table 6-2.

The PSHA is used to calculate the annual frequency of exceeding a specified ground motion level. Results of the PSHA are typically presented in terms of ground motion as a function of annual exceedance probability. Figure 6-1 shows the total hazard curve plotted for the lower bound  $V_{s30}$  of 902 ft/s (275 m/s), which resulted in the highest mean PGA. At the 10,000-year return period, the hazard is controlled by the background earthquake from the CP areal source zone. Crustal faults have little effect on the total hazard due to the distance from the site. The Uniform Hazard Spectra (UHS) was computed for the 10,000 and 2,500-year return periods and for each of the  $V_{s30}$  values. The UHS are shown in Figure 6-2.

The hazard was deaggregated to evaluate the magnitude and distance contributions to the mean PGA for each  $V_{s30}$  value. The deaggregation of the hazard allows the probability density to be calculated for selected distance and magnitude bins. The deaggregated hazard is shown on Figures 6-3 through 6-5. The plots also include mean magnitude, mean distance, and mean epsilon values. Based on the deaggregation, the hazard is generally dominated by earthquakes greater than  $M_w$  5.0 located less than 19 miles (30 km) from the site. In summary, the deaggregation results for the three shear wave velocities are as follows:

- For a  $V_{s30} = 902$  ft/s (275 m/s), the mean magnitude was calculated to be  $M_w$  5.8 at a mean distance of 26 km (Figure 6-3), and the modal magnitude was calculated to be  $M_w$  5.5 at modal distance of 12.4 miles (20 km).
- For a  $V_{s30} = 1,348$  ft/s (420 m/s), the mean magnitude was calculated to be  $M_w$  5.8 at a mean distance of 25 km (Figure 6-4), and the modal magnitude was calculated to be  $M_w$  5.5 at modal distance of 12.4 miles (20 km).
- For a  $V_{s30} = 1,857$  ft/s (566 m/s), the mean magnitude was calculated to be  $M_w$  5.8 at a mean distance of 25 km (Figure 6-5), and the modal magnitude was calculated to be  $M_w$  5.5 at modal distance of 12.4 miles (20 km).

## 7.0 DETERMINISTIC SEISMIC HAZARD ANALYSIS

The DSHA can be described as a procedure of four steps (Kramer 1996):

1. Identification and characterization of earthquake sources capable of producing significant ground motions at the site
2. Selection of source to site distance parameter for each source zone, consistent with attenuation relationship selected
3. Selection of controlling earthquake
4. Hazard at the site is formally defined, in terms of ground motions produced at the site by the controlling earthquake

Calculations for this report were performed using a spreadsheet developed by PEER (2015). The Excel spreadsheet calculates the weighted average of the natural logarithm of the spectral values from the GMPEs. The same GMPEs and weighting used in the PSHA were used in the DSHA. The deterministic evaluation also excludes the Idriss (2014) relationship due to the limitation on minimum  $V_{S30}$ .

DSHA methods require source parameters for location, geometry, orientation, sense of slip, and maximum magnitude. No information is required on recurrence or slip rates. Thus for the DSHA, potential sources were evaluated only as 100 percent active (or 100 percent inactive) with no consideration of slip rate. There are no mapped faults within 50 km of the site. The two closest faults to the site are the Unnamed Faults of the El Malpais Lava Field and the Unnamed Fault of Bonita Canyon, which are both approximately 90 km from the site. However, both of these faults are Class B faults and were each assigned a probability of activity of 0.5. Therefore, these faults were not included in the deterministic analysis. The seismic sources evaluated in the DSHA included: the unsegmented Nacimiento fault, the Interbasin faults on the Llano de Albuquerque, the unsegmented Jemez-San Ysidro fault, and the unsegmented San Felipe fault. These unsegmented faults are approximately 150 km from the site, with estimated rupture lengths greater than 80 km.

The lowest  $V_{S30}$  of 275 m/s was used in the DSHA calculations.

### 7.1 Deterministic Inputs

The input parameters for the NGA-West 2 relationships are summarized in Table 7-1.

### 7.2 Deterministic Seismic Hazard Analysis Results

The weighted average of the median and 84<sup>th</sup> percentile (median+1 $\sigma$ ) acceleration values for 5 percent damping are summarized in Table 7-2. The deterministic spectra for the median and 84<sup>th</sup> percentile are shown in Figure 7-1. The DSHA results for the four considered faults are similar with PGA values for the 84<sup>th</sup> percentile ranging from 0.04 to 0.07 g, with the Nacimiento fault resulting in ground motions only slightly higher than the other three faults.

## 8.0 RESULTS AND COMPARISON WITH PREVIOUS STUDIES

The results of this site-wide SHA indicate the mean PGA for long-term conditions is estimated to range from 0.25 g to 0.30 g. The PGA values are associated with an average return period of 10,000 years, or a probability of exceedance of 2 percent to 10 percent for a design life of 200 to 1,000 years, respectively. The  $V_{S30}$  values used for the analysis ranged from 902 ft/s to 1,857 ft/s (275 m/s to 566 m/s). Selection of the PGA or a pseudostatic coefficient used for long-term design of the repository shall be performed during design and be based on the results presented in Table 6-2. For all considered  $V_{S30}$  values, the controlling earthquake is estimated as magnitude 5.5 at a distance of 12.4 miles (20 km).

Comparing the DSHA results to the PSHA results for a  $V_{S30}$  of 275 m/s (Figure 8-1), the UHS for the 10,000-year return period is well above the 84<sup>th</sup> percentile of the Nacimiento fault, which had the highest ground motions of the sources considered in the DSHA. The 2,475-year return period UHS is above the 84<sup>th</sup> percentile for the Nacimiento fault for spectral periods up to 2 seconds. Overall, the PGA from the 10,000-year event for a  $V_{S30}$  of 275 m/s is 0.30 g.

Results of this site-specific PSHA were compared to previous analyses conducted for the site by LLNL (1994) and the PGA and associated earthquake selected by NRC (1997). LLNL (1994) developed PGA hazard curves for a random (or background) earthquake since the site is not near any significant structure. The maximum PGA reported by LLNL (1994) was 0.22 g for the 10,000-year return period and a magnitude of 7.0. Based on the results of LLNL's (1994) regional study and considering conditions at the site, NRC (1997) selected site-specific PGA of 0.196 g for a magnitude of 6.25. Results of the LLNL analyses indicate a deterministically derived PGA of 0.196 g for a magnitude 6.25 event. This Both LLNL (1994) and NRC (1997) values for PGA is are lower than the 10,000-year return period PGA calculated in this study (0.25 g to 0.30 g) for the 10,000-year return period for the three considered  $V_{S30}$  values and considering background seismicity. It is speculated that the PGA results reported by LLNL (1994) was for soft rock ( $V_{S30}$  of 760 m/s) and not the existing subsurface of alluvium, as was used in this study.

Additionally, results of this site-specific PSHA were compared to USGS 2014 NSHMP gridded hazard curves. The USGS 2014 NSHMP indicate a PGA of 0.08 g for a return period of 2,475 years at a  $V_{S30}$  of 760 m/s, which is less than this study's calculation of 0.14 to 0.18 g for the same return period and  $V_{S30}$  of 275 to 566 m/s, respectively.

## 9.0 REFERENCES

- Abrahamson, N.A., W.J. Silva, and R. Kamai, 2014. *Summary of the ASK14 Ground-Motion Relation for Active Crustal Regions*. Earthquake Spectra. Volume 30, Issue 3. August.
- Boore, D. M., 2004. Estimating VS(30) (or NEHRP Site Classes) from shallow velocity models (depths < 30m), Bull. Seismo. Soc. Am., 94(2):591–597.
- Boore, P.M., J.P. Stewart, E. Seyhan, and G.M. Atkinson, 2014. *NGA-West 2 Equations for Predicting PGA, PGV, and 5%-Damped PSA for Shallow Crustal Earthquakes*. Earthquake Spectra. Volume 30, Issue 3. August.
- Bott, J.D.J., Wong, I.G., and Ake, J., 2003. Contemporary seismicity, 1983–1993, and its implications to seismic hazard in the Central Front Range, Colorado. In *Engineering Geology in Colorado: Contributions, Trends, and Case Histories*, ed. D. Boyer, P. Santi, and W. Rogers. Association of Engineering Geologists special publication 15, Colorado Geological Survey special publication 55, 18 pps.
- Campbell, K. W., and Y. Bozorgnia, 2014. *NGA-West2 Ground Motion Model for the Average Horizontal Components of PGA, PGV, and 5%-Damped Linear Acceleration Response Spectra*. Earthquake Spectra. Volume 30, Issue 3. August.
- [Canonie Environmental, 1987. Reclamation Engineering Services: Geohydrologic Report. Church Rock Site, Gallup, New Mexico.](#)
- Canonie Environmental (Canonie), 1991. Tailings Reclamation Plan, As Approved by NRC March 1, 1991, License No. SUA-1475. Prepared for United Nuclear Corporation. August.
- Chamberlin, R.M., S.M. Cather, O.J. Anderson, and G.E. Jones, 1994. Reconnaissance geologic map of the Quemado 30 x 60 minute quadrangle, Catron County, New Mexico: New Mexico Bureau of Mines and Mineral Resources Open File Report 406, 29 p. pamphlet, 1 sheet, scale 1:100,000.
- Chiou, B. S., and R.R. Youngs, 2014. *Update of the Chiou and Youngs NGA Model for the Average Horizontal Component of Peak Ground Motion and Response Spectra*. Earthquake Spectra. Volume 30, Issue 3. August.
- ~~Canonie Environmental, 1987. Reclamation Engineering Services: Geohydrologic Report. Church Rock Site, Gallup, New Mexico.~~
- Cornell, C.A., 1968. *Engineering seismic risk analysis*, Bulletin of Seismological Society of America, v.58 p. 1583-1606.
- Haller, K.M., and Personius, S.F., compilers, 2015, Fault number 2120, Hubbell Spring fault, in Quaternary fault and fold database of the United States: U.S. Geological Survey website, <https://earthquakes.usgs.gov/hazards/qfaults>, accessed 08/09/2017 12:28 PM.
- Haller, K.M., Kelson, K.I., and Koning, D.J., compilers, 2015a, Fault number 2008, Pajarito fault zone, in Quaternary fault and fold database of the United States: U.S. Geological Survey website, <https://earthquakes.usgs.gov/hazards/qfaults>, accessed 08/09/2017 12:40 PM.
- Haller, K.M., Personius, S.F., Olig, S.S., and McCalpin, J.P., compilers, 2015b, Fault number 2038, County Dump fault, in Quaternary fault and fold database of the United States: U.S. Geological Survey website, <https://earthquakes.usgs.gov/hazards/qfaults>, accessed 08/09/2017 12:21 PM.
- Idriss I.M., 2014. *An NGA Empirical Model for Estimating the Horizontal Spectral Values Generated By Shallow Crustal Earthquakes*. Earthquake Spectra. Volume 30, Issue 3. August.
- Jochems, A.P., and Personius, S.F., compilers, 2016a, Fault number 2117, Unnamed faults on the Llano de Manzano, in Quaternary fault and fold database of the United States: U.S. Geological Survey website, <https://earthquakes.usgs.gov/hazards/qfaults>, accessed 08/09/2017 12:59 PM.
- Jochems, A.P., and Personius, S.F., compilers, 2016b, Fault number 2121, Intrabasin faults on the Llano de Albuquerque, in Quaternary fault and fold database of the United States: U.S. Geological Survey website, <https://earthquakes.usgs.gov/hazards/qfaults>, accessed 08/09/2017 12:28 PM.

- Jochems, A.P., Kelson, K.I., and Personius, S.F., compilers, 2016, Fault number 2029a, Jemez-San Ysidro fault, Jemez section, in Quaternary fault and fold database of the United States: U.S. Geological Survey website, <https://earthquakes.usgs.gov/hazards/qfaults>, accessed 08/09/2017 12:29 PM.
- Kelson, K.I., compiler, 1996, Fault number 2024, Nambe fault, in Quaternary fault and fold database of the United States: U.S. Geological Survey website, <https://earthquakes.usgs.gov/hazards/qfaults>, accessed 08/09/2017 12:37 PM.
- Kelson, K.I., and Jochems, A.P., compilers, 2015, Fault number 2001, Gallina fault, in Quaternary fault and fold database of the United States: U.S. Geological Survey website, <https://earthquakes.usgs.gov/hazards/qfaults>, accessed 08/09/2017 12:26 PM.
- Kelson, K.I., and Jochems, A.P., compilers, 2016a, Fault number 2023, Picuris-Pecos fault, in Quaternary fault and fold database of the United States: U.S. Geological Survey website, <https://earthquakes.usgs.gov/hazards/qfaults>, accessed 09/06/2017 04:37 PM.
- Kelson, K.I., and Jochems, A.P., compilers, 2016b, Fault number 2033a, Tijeras-Cañoncito fault system, Galisteo section, in Quaternary fault and fold database of the United States: U.S. Geological Survey website, <https://earthquakes.usgs.gov/hazards/qfaults>, accessed 08/09/2017 12:55 PM.
- Kelson, K.I., and Jochems, A.P., compilers, 2016c, Fault number 2033b, Tijeras-Cañoncito fault system, Canyon section, in Quaternary fault and fold database of the United States: U.S. Geological Survey website, <https://earthquakes.usgs.gov/hazards/qfaults>, accessed 08/09/2017 12:55 PM.
- Kelson, K.I., and Personius, S.F., compilers, 1996, Fault number 2010, Pojoaque fault zone, in Quaternary fault and fold database of the United States: U.S. Geological Survey website, <https://earthquakes.usgs.gov/hazards/qfaults>, accessed 08/09/2017 12:41 PM.
- Kelson, K.I., Haller, K.M., Kirkham, R.M., and Machette, M.N., compilers, 2015a, Fault number 2017b, Southern Sangre de Cristo fault, Urraca section, in Quaternary fault and fold database of the United States: U.S. Geological Survey website, <https://earthquakes.usgs.gov/hazards/qfaults>, accessed 08/09/2017 12:51 PM.
- Kelson, K.I., Haller, K.M., Kirkham, R.M., and Machette, M.N., compilers, 2015b, Fault number 2017c, Southern Sangre de Cristo fault, Questa section, in Quaternary fault and fold database of the United States: U.S. Geological Survey website, <https://earthquakes.usgs.gov/hazards/qfaults>, accessed 08/09/2017 12:53 PM.
- Kelson, K.I., Haller, K.M., and Koning, D.J., compilers, 2015c, Fault number 2007, Embudo fault, in Quaternary fault and fold database of the United States: U.S. Geological Survey website, <https://earthquakes.usgs.gov/hazards/qfaults>, accessed 08/09/2017 12:24 PM.
- Kelson, K.I., Haller, K.M., Koning, D.J., Kirkham, R.M., and Machette, M.N., compilers, 2015d, Fault number 2017e, Southern Sangre de Cristo fault, Cañon section, in Quaternary fault and fold database of the United States: U.S. Geological Survey website, <https://earthquakes.usgs.gov/hazards/qfaults>, accessed 08/09/2017 12:54 PM.
- Kelson, K.I., Jochems, A.P., and Personius, S.F., compilers, 2015e, Fault number 2002a, Nacimiento fault, northern section, in Quaternary fault and fold database of the United States: U.S. Geological Survey website, <https://earthquakes.usgs.gov/hazards/qfaults>, accessed 08/09/2017 12:36 PM.
- Kelson, K.I., Jochems, A.P., and Personius, S.F., compilers, 2015f, Fault number 2002b, Nacimiento fault, southern section, in Quaternary fault and fold database of the United States: U.S. Geological Survey website, <https://earthquakes.usgs.gov/hazards/qfaults>, accessed 08/09/2017 12:37 PM.
- Kelson, K.I., Kirkham, R.M., and Machette, M.N., compilers, 1998, Fault number 2017d, Southern Sangre de Cristo fault, Hondo section, in Quaternary fault and fold database of the United States: U.S. Geological Survey website, <https://earthquakes.usgs.gov/hazards/qfaults>, accessed 08/09/2017 12:53 PM.
- Kelson, K.I., Kirkham, R.M., Machette, M.N., and Koning, D.J., compilers, 2015g, Fault number 2017a, Southern Sangre de Cristo fault, San Pedro Mesa section, in Quaternary fault and fold database of the United States: U.S. Geological Survey website, <https://earthquakes.usgs.gov/hazards/qfaults>, accessed 08/09/2017 12:50 PM.



- Kelson, K.I., Personius, S.F., Haller, K.M., Koning, D.J., and Jochems, A.P., compilers, 2015h, Fault number 2029b, Jemez-San Ysidro fault, San Ysidro section, in Quaternary fault and fold database of the United States: U.S. Geological Survey website, <https://earthquakes.usgs.gov/hazards/qfaults>, accessed 08/09/2017 12:29 PM.
- Kirkham, R.M., compiler, 2012, Fault number 2321c, Northern Sangre de Cristo fault, Blanca section, in Quaternary fault and fold database of the United States: U.S. Geological Survey website, <https://earthquakes.usgs.gov/hazards/qfaults>, accessed 08/09/2017 12:39 PM.
- Kirkham, R.M., and Haller, K.M., compilers, 2012a, Fault number 2321b, Northern Sangre de Cristo fault, Zapata section, in Quaternary fault and fold database of the United States: U.S. Geological Survey website, <https://earthquakes.usgs.gov/hazards/qfaults>, accessed 08/09/2017 12:39 PM.
- Kirkham, R.M., and Haller, K.M., compilers, 2012b, Fault number 2321d, Northern Sangre de Cristo fault, San Luis section, in Quaternary fault and fold database of the United States: U.S. Geological Survey website, <https://earthquakes.usgs.gov/hazards/qfaults>, accessed 08/09/2017 12:40 PM.
- Kirkham, R.M., and Haller, K.M., compilers, 2015, Fault number 2321a, Northern Sangre de Cristo fault, Crestone section, in Quaternary fault and fold database of the United States: U.S. Geological Survey website, <https://earthquakes.usgs.gov/hazards/qfaults>, accessed 08/09/2017 12:39 PM.
- Koning, D.J., Haller, K.M., and Jochems, A.P., compilers, 2015, Fault number 2029c, Jemez-San Ysidro fault, Calabacillas section, in Quaternary fault and fold database of the United States: U.S. Geological Survey website, <https://earthquakes.usgs.gov/hazards/qfaults>, accessed 08/09/2017 12:30 PM.
- Kramer, S.L., 1996. *Geotechnical Earthquake Engineering, Upper Saddle River, New Jersey*, Prentice Hall.
- [Lawrence Livermore National Laboratory \(LLNL\), 1994. Seismic Hazard Analysis of Title II Reclamation Plans. Prepared for US Nuclear Regulatory Commission,](#)
- Levish, D.R., U.R. Vetter, J.P. Ake, and L.A. Piety, 1992. Seismotectonic study for Black Rock Dam, Bureau of Indian Affairs, Pueblo of Zuni, New Mexico: Bureau of Reclamation Seismotectonic Report 923, 62 p.
- Machette, M.N., and Chamberlin, R.M., compilers, 2015, Fault number 2108b, Socorro Canyon fault zone, southern section, in Quaternary fault and fold database of the United States: U.S. Geological Survey website, <https://earthquakes.usgs.gov/hazards/qfaults>, accessed 08/09/2017 12:50 PM.
- Machette, M.N., and Chamberlin, R.M., compilers, 2016, Fault number 2109b, La Jencia fault, southern section, in Quaternary fault and fold database of the United States: U.S. Geological Survey website, <https://earthquakes.usgs.gov/hazards/qfaults>, accessed 08/09/2017 12:32 PM.
- Machette, M.N., and Jochems, A.P., compilers, 2015a, Fault number 2053a, San Andres Mountains fault, northern section, in Quaternary fault and fold database of the United States: U.S. Geological Survey website, <https://earthquakes.usgs.gov/hazards/qfaults>, accessed 08/09/2017 12:44 PM.
- Machette, M.N., and Jochems, A.P., compilers, 2015b, Fault number 2053b, San Andres Mountains fault, central section, in Quaternary fault and fold database of the United States: U.S. Geological Survey website, <https://earthquakes.usgs.gov/hazards/qfaults>, accessed 08/09/2017 12:46 PM.
- Machette, M.N., and Jochems, A.P., compilers, 2015c, Fault number 2053c, San Andres Mountains fault, southern section, in Quaternary fault and fold database of the United States: U.S. Geological Survey website, <https://earthquakes.usgs.gov/hazards/qfaults>, accessed 08/09/2017 12:47 PM.
- Machette, M.N., and Jochems, A.P., compilers, 2015d, Fault number 2056a, Jornada Draw fault, northern section, in Quaternary fault and fold database of the United States: U.S. Geological Survey website, <https://earthquakes.usgs.gov/hazards/qfaults>, accessed 09/07/2017 05:27 PM.

- Machette, M.N., and Jochems, A.P., compilers, 2015e, Fault number 2056b, Jornada Draw fault, central section, in Quaternary fault and fold database of the United States: U.S. Geological Survey website, <https://earthquakes.usgs.gov/hazards/qfaults>, accessed 09/07/2017 05:27 PM.
- Machette, M.N., and Jochems, A.P., compilers, 2015f, Fault number 2056c, Jornada Draw fault, southern section, in Quaternary fault and fold database of the United States: U.S. Geological Survey website, <https://earthquakes.usgs.gov/hazards/qfaults>, accessed 09/07/2017 05:27 PM.
- Machette, M.N., and Jochems, A.P., compilers, 2016a, Fault number 2131, Unnamed faults along San Mateo Mountains, in Quaternary fault and fold database of the United States: U.S. Geological Survey website, <https://earthquakes.usgs.gov/hazards/qfaults>, accessed 08/09/2017 12:56 PM.
- Machette, M.N., and Jochems, A.P., compilers, 2016b, Fault number 2136, Hickman fault, in Quaternary fault and fold database of the United States: U.S. Geological Survey website, <https://earthquakes.usgs.gov/hazards/qfaults>, accessed 08/09/2017 11:33 AM.
- Machette, M.N., and Jochems, A.P., compilers, 2016c, Fault number 2140, Cebollita Mesa fault, in Quaternary fault and fold database of the United States: U.S. Geological Survey website, <https://earthquakes.usgs.gov/hazards/qfaults>, accessed 08/09/2017 11:43 AM.
- Machette, M.N., and Jochems, A.P., compilers, 2016d, Fault number 2144, Unnamed fault of Bonita Canyon, in Quaternary fault and fold database of the United States: U.S. Geological Survey website, <https://earthquakes.usgs.gov/hazards/qfaults>, accessed 08/09/2017 11:38 AM.
- Machette, M.N., and Jochems, A.P., compilers, 2016e, Fault number 2145, Continental Divide fault, in Quaternary fault and fold database of the United States: U.S. Geological Survey website, <https://earthquakes.usgs.gov/hazards/qfaults>, accessed 08/09/2017 11:38 AM.
- Machette, M.N., and Jochems, A.P., compilers, 2016f, Fault number 2146, Unnamed faults of El Malpais lava field, in Quaternary fault and fold database of the United States: U.S. Geological Survey website, <https://earthquakes.usgs.gov/hazards/qfaults>, accessed 08/09/2017 11:40 AM.
- Machette, M.N., Chamberlin, R.M., and Jochems, A.P., compilers, 2016a, Fault number 2109a, La Jencia fault, northern section, in Quaternary fault and fold database of the United States: U.S. Geological Survey website, <https://earthquakes.usgs.gov/hazards/qfaults>, accessed 08/09/2017 12:31 PM.
- Machette, M.N., Jochems, A.P., and Chamberlin, R.M., compilers, 2016b, Fault number 2108a, Socorro Canyon fault zone, northern section, in Quaternary fault and fold database of the United States: U.S. Geological Survey website, <https://earthquakes.usgs.gov/hazards/qfaults>, accessed 08/09/2017 12:49 PM.
- Pacific Earthquake Engineering Research Center (PEER), 2015. Weighted Average of 2014 NGA West-2 GMPEs: PEER Website, <http://peer.berkeley.edu/ngawest2/databases/>.
- Pearthree, P.A., compiler, 1997, Fault number 991, Bright Angel fault zone, in Quaternary fault and fold database of the United States: U.S. Geological Survey website, <https://earthquakes.usgs.gov/hazards/qfaults>, accessed 08/09/2017 11:41 AM.
- Pearthree, P.A., compiler, 1998a, Fault number 1014, Concho fault, in Quaternary fault and fold database of the United States: U.S. Geological Survey website, <https://earthquakes.usgs.gov/hazards/qfaults>, accessed 08/09/2017 12:21 PM.
- Pearthree, P.A., compiler, 1998b, Fault number 1015, Coyote Wash fault, in Quaternary fault and fold database of the United States: U.S. Geological Survey website, <https://earthquakes.usgs.gov/hazards/qfaults>, accessed 08/09/2017 12:23 PM.
- Pearthree, P.A., compiler, 1998c, Fault number 1016, Vernon fault zone, in Quaternary fault and fold database of the United States: U.S. Geological Survey website, <https://earthquakes.usgs.gov/hazards/qfaults>, accessed 08/09/2017 01:00 PM.

- Pearthree, P.A., compiler, 1998d, Fault number 1017, Leupp faults, in Quaternary fault and fold database of the United States: U.S. Geological Survey website, <https://earthquakes.usgs.gov/hazards/qfaults>, accessed 08/09/2017 12:33 PM.
- Personius, S.F., and Haller, K.M., compilers, 2015, Fault number 2046, Zia fault, in Quaternary fault and fold database of the United States: U.S. Geological Survey website, <https://earthquakes.usgs.gov/hazards/qfaults>, accessed 08/09/2017 01:02 PM.
- Personius, S.F., and Jochems, A.P., compilers, 2015, Fault number 2123, Santa Fe fault, in Quaternary fault and fold database of the United States: U.S. Geological Survey website, <https://earthquakes.usgs.gov/hazards/qfaults>, accessed 08/09/2017 12:49 PM.
- Personius, S.F., and Jochems, A.P., compilers, 2016a, Fault number 2032, La Bajada fault, in Quaternary fault and fold database of the United States: U.S. Geological Survey website, <https://earthquakes.usgs.gov/hazards/qfaults>, accessed 08/09/2017 12:31 PM.
- Personius, S.F., and Jochems, A.P., compilers, 2016b, Fault number 2039, Sand Hill fault zone, in Quaternary fault and fold database of the United States: U.S. Geological Survey website, <https://earthquakes.usgs.gov/hazards/qfaults>, accessed 08/09/2017 12:43 PM.
- Personius, S.F., and Jochems, A.P., compilers, 2016c, Fault number 2048, Unnamed faults near Star Heights, in Quaternary fault and fold database of the United States: U.S. Geological Survey website, <https://earthquakes.usgs.gov/hazards/qfaults>, accessed 08/09/2017 12:58 PM.
- Personius, S.F., and Jochems, A.P., compilers, 2016d, Fault number 2049, Unnamed faults near Albuquerque Volcanoes, in Quaternary fault and fold database of the United States: U.S. Geological Survey website, <https://earthquakes.usgs.gov/hazards/qfaults>, accessed 08/09/2017 12:57 PM.
- Personius, S.F., and Jochems, A.P., compilers, 2016e, Fault number 2110, West Joyita fault zone, in Quaternary fault and fold database of the United States: U.S. Geological Survey website, <https://earthquakes.usgs.gov/hazards/qfaults>, accessed 08/09/2017 01:01 PM.
- Personius, S.F., and Jochems, A.P., compilers, 2016f, Fault number 2113, Loma Pelada fault, in Quaternary fault and fold database of the United States: U.S. Geological Survey website, <https://earthquakes.usgs.gov/hazards/qfaults>, accessed 08/09/2017 12:34 PM.
- Personius, S.F., and Jochems, A.P., compilers, 2016g, Fault number 2119, Manzano fault, in Quaternary fault and fold database of the United States: U.S. Geological Survey website, <https://earthquakes.usgs.gov/hazards/qfaults>, accessed 08/09/2017 12:34 PM.
- Personius, S.F., and Jochems, A.P., compilers, 2016i, Fault number 2135, McCormick Ranch faults, in Quaternary fault and fold database of the United States: U.S. Geological Survey website, <https://earthquakes.usgs.gov/hazards/qfaults>, accessed 08/09/2017 12:35 PM.
- Personius, S.F., and Jochems, A.P., compilers, 2016j, Fault number 2142, Faults near Cochiti Pueblo, in Quaternary fault and fold database of the United States: U.S. Geological Survey website, <https://earthquakes.usgs.gov/hazards/qfaults>, accessed 08/09/2017 12:26 PM.
- Personius, S.F., Jochems, A.P., and Kelson, K.I., compilers, 2016a, Fault number 2030a, San Felipe fault zone, Santa Ana section, in Quaternary fault and fold database of the United States: U.S. Geological Survey website, <https://earthquakes.usgs.gov/hazards/qfaults>, accessed 08/09/2017 12:42 PM.
- Personius, S.F., Kelson, K.I., and Jochems, A.P., compilers, 2016b, Fault number 2030b, San Felipe fault zone, Algodones section, in Quaternary fault and fold database of the United States: U.S. Geological Survey website, <https://earthquakes.usgs.gov/hazards/qfaults>, accessed 08/09/2017 12:42 PM.
- Petersen, M.D., M.O. Moschetti, P.M. Powers, C.S. Mueller, K.M. Haller, A.D. Frankel, Y. Aeng, S. Rezaeian, S.C. Harmsen, O.S. Boyd, N. Field, R. Chen, K.S. Rukstales, N. Luco, R.S. Wheeler, R.A. Williams, and A.H. Olsen, 2014.

*Documentation for the 2014 Update of the United States National Seismic Hazard Maps.* United States Geological Survey Open-File Report 2014-1091.

- Petersen, Mark D., et al. 2016 one-year seismic hazard forecast for the Central and Eastern United States from induced and natural earthquakes. No. 2016-1035. US Geological Survey, 2016.
- Thomas, P., I. Wong, and N. Abrahamson, 2010. *Verification of Probabilistic Seismic Hazard Analysis Computer Programs*. May.
- [Sanford, A.R., K.H. Olsen, K.H. and L.H. Jaksha, L.H., 1981. Earthquakes in New Mexico, 1849-1977. New Mexico Bureau of Mines and Mineral Resources Circular 171, 20 pp.](#)
- Sawyer, D.A., and Minor, S.A., 2006, Geologic setting of the La Bajada constriction and Cochiti Pueblo area, in Minor, S.A., ed., *The Cerrillos uplift, the La Bajada constriction, and hydrogeologic framework of the Santo Domingo basin, Rio Grande rift, New Mexico: U.S. Geological Survey, Professional Paper 1720*, p. 3-23.
- Sbar, M.L., 1982. *Delineation and Interpretation of Seismotectonic Domains in Western North America*. Journal of Geophysical Research, v. 87, no. B5, p. 3919-3928. May.
- Stepp, J.C., 1972. *Analysis of the completeness of the earthquake hazard sample in the Puget Sound area and its effects on statistical estimates of earthquake hazard*, Proc. Intern. Conf. Microzonation for Safer Construct. Res. Appl., Seattle, Washington 2, 897-909.
- U.S. Geological Survey (USGS), 2017. *Quaternary fault and fold database for the United States*, accessed September 2017, from USGS web site: <http://earthquake.usgs.gov/hazards/qafaults>.
- US Nuclear Regulatory Commission (NRC), 1997. *Seismic Evaluation of Church Rock Tailings Impoundments*, September 17.
- US Nuclear Regulatory Commission (NRC). 2013. *10 CFR Appendix A to Part 100 – Seismic and Geologic Siting Criteria for Nuclear Power Plants*. <http://www.nrc.gov/reading-rm/doc-collections/cfr/part100/part100-appa.html>. Accessed March.
- US Nuclear Regulatory Commission (NRC), U.S. Department of Energy (DOE), and Electric Power Research Institute (EPRI), 2012. (CEUS-SSCn) *Technical Report: Central and Eastern United States Seismic Source Characterization for Nuclear Facilities*.
- Weichert, D., 1980. *Estimation of the earthquake recurrence parameters for unequal observation periods for different magnitudes*. Bulletin of the Seismological Society of America 70: 1337-1346.
- Wells, D.L. and K.J. Coppersmith, 1994. "New empirical relationships among magnitude, rupture length, rupture width, rupture area and surface displacement." Bulletin of the Seismological Society of America, Vol. 84, No. 4, pp. 974-1002.
- [Willis, B., 1929, Geologic Structures: N.Y., McCraw-Hill, 518 p.](#)
- Wills, C.J. and K.B. Clahan, 2006. Developing a map of geologically defined site-conditions categories for California: Bulletin of the Seismological Society of America, accepted for publication, anticipated publication in August 2006 issue.
- [Wong, I.G., Cash, D.J., and Jaksha, L.H., 1984. The Crownpoint, New Mexico, Earthquakes of 1976 and 1977. Bulletin of the Seismological Society of America, Vol. 74, No. 6, pp. 2435-2440. December 1984.](#)
- Wong, I.G., and J.R. Humphrey, 1989. *Contemporary seismicity, faulting, and the state of stress in the Colorado Plateau*, Geological Society of America Bulletin 101: 1127-1146.
- Wong, I., K. Kelson, S. Olig, T. Kolbe, M. Hemphill Haley, J. Bott, R. Green, H. Kanakari, J. Sawyer, W. Silva, C. Stark, C. Haraden, C. Fenton, J. Unruh, J. Gardner, S. Reneau, and L. House, 1995. *Seismic hazards evaluation of the Los Alamos National Laboratory: Technical report to Los Alamos National Laboratory, Los Alamos, New Mexico*. February 24. 3 volumes, 12 pls., 16 appendix.
- Wong, I.G. and S.S. Olig. 1998. *Seismic Hazards in the Basin and Range Province: Perspectives from Probabilistic Analyses*. In *Western States Seismic Policy Council Proceedings*. p. 110-127.

Woodward, L.A., 1987, Geology and mineral resources of Sierra Nacimiento and vicinity, New Mexico: New Mexico Bureau of Mines and Mineral Resources Memoir 42, 84 p., 1 pl., scale 1:100,000.

## TABLES

**Table 3-1: Time Periods for Complete Event Reporting**

Magnitude Range	Period of Complete Reporting	
2.5≤M<3.0	2000	2016
3≤M<3.5	1985	2016
3.5≤M<4.0	1965	2016
4.0≤M<4.5	1965	2016
4.5≤M<5.0	1960	2016
5.0≤M	1885	2016

**Table 3-2: Colorado Plateau – Magnitude Bins and Cumulative N\* Values**

Magnitude Bin	Cumulative N* value	Cumulative Observed Counts
2.5≤M<3.0	149.39	142
3≤M<3.5	169.44	160
3.5≤M<4.0	110.70	103
4.0≤M<4.5	42.87	40
4.5≤M<5.0	15.97	15
5.0≤M<5.5	12.18	11
5.5≤M<6.0	5.92	5
6.0≤M<6.5	2.41	2
6.5≤M<7.0	1.21	1

**Table 4-1: Faults Included in Analysis**

Fault Name	Distance from Site	Maximum Magnitude
Cebollita Mesa	107	6.3
Continental Divide	101	6.5
Hickman	130	6.1
Nacimiento	124	7.4
Unnamed fault of Bonita Canyon	88	6.1
Unnamed faults of El Malpais lava field	89	6.7

Table 4-2: PSHA Input Parameters

No.	Fault	Fault Number <sup>(1)</sup>	Distance from Site (km)	Rupture Model	Probability of Activity	Sense of Slip	Time Since Most Recent Deformation	Max Rupture Length (km)	Seismogenic Depth (km)	Dip	M <sub>max</sub> <sup>(2)</sup>	Weighting	Slip Rate (mm/yr)	Weighted Mean of Slip Rate	Recurrence Model	b-value
1	Bright Angel fault zone	991	321	Unsegmented	1	N	<1.6 Ma	74	25	45 SE	7.0	0.2	0.001 (0.2)	0.10	Characteristic (0.7) Maximum Magnitude (0.3)	0.84
										66 SE	7.3	0.6	0.1 (0.6)			
										87 SE	7.6	0.2	0.2 (0.2)			
2	Cebollita Mesa fault	2140	107	Unsegmented	1	N	<15 ka	13	25	35 W	6.3	0.2	0.001 (0.2)	0.10	Characteristic (0.7) Maximum Magnitude (0.3)	0.84
										50 W	6.6	0.6	0.1 (0.6)			
										65 W	6.9	0.2	0.2 (0.2)			
3	Concho fault	1014	160	Unsegmented	1	N/SS	<750 ka	39	25	35 SE	6.8	0.2	0.019 (0.2)	0.03	Characteristic (0.7) Maximum Magnitude (0.3)	0.84
										50 SE	7.1	0.6	0.03 (0.6)			
										65 SE	7.4	0.2	0.04 (0.2)			
4	Continental Divide fault (Class B)	2145	101	Unsegmented	1	N	<1.6 Ma	17	25	35 SE	6.5	0.2	0.001 (0.2)	0.10	Characteristic (0.7) Maximum Magnitude (0.3)	0.84
										50 SE	6.8	0.6	0.1 (0.6)			
										65 SE	7.1	0.2	0.2 (0.2)			
5	County Dump fault	2038	160	Unsegmented	1	N	<130 ka	35	25	75 E	6.7	0.2	0.015 (0.2)	0.02	Characteristic (0.7) Maximum Magnitude (0.3)	0.84
										80 E	7.0	0.6	0.02 (0.6)			
										85 E	7.3	0.2	0.024 (0.2)			
6	Coyote Wash fault	1015	158	Unsegmented	1	N/SS	<750 ka	42	25	35 SW	6.8	0.2	0.001 (0.2)	0.10	Characteristic (0.7) Maximum Magnitude (0.3)	0.84
										50 SW	7.1	0.6	0.1 (0.6)			
										65 SW	7.4	0.2	0.2 (0.2)			
7	Embudo fault	2007	233	Unsegmented	1	SS/N	<130 ka	40	25	90	6.7	0.2	0.001 (0.2)	0.10	Characteristic (0.7) Maximum Magnitude (0.3)	0.84
											7.0	0.6	0.1 (0.6)			
											7.3	0.2	0.2 (0.2)			
8	Faults near Cochiti Pueblo	2142	183	Unsegmented	1	N	<1.6 Ma	32	25	60 W	6.7	0.2	0.042 (0.2)	0.11	Characteristic (0.7) Maximum Magnitude (0.3)	0.84
										65 W	7.0	0.6	0.11 (0.6)			
										75 W	7.3	0.2	0.17 (0.2)			
9	Gallina fault	2001	157	Unsegmented	1	N	<1.6 Ma	39	25	70 E	6.7	0.2	0.001 (0.2)	0.10	Characteristic (0.7) Maximum Magnitude (0.3)	0.84
										90	7.0	0.6	0.1 (0.6)			
										70 W	7.3	0.2	0.2 (0.2)			
10	Hickman fault	2136	130	Unsegmented	1	N	<130 ka	9	25	60 W	6.2	0.2	0.001 (0.2)	0.10	Characteristic (0.7) Maximum Magnitude (0.3)	0.84
										75 W	6.5	0.6	0.1 (0.6)			
										90 W	6.8	0.2	0.2 (0.2)			
11	Hubbell Spring fault	2120	192	Unsegmented	1	N	<15 ka	74	25	48 W	7.0	0.2	0.2 (0.2)	0.60	Characteristic (0.7) Maximum Magnitude (0.3)	0.84
										66 W	7.3	0.6	0.6 (0.6)			
										85 W	7.6	0.2	1 (0.2)			
12	Intrabasin faults on the Llano de Albuquerque	2121	158	Unsegmented	1	N	<750 ka	101	25	50 E	7.1	0.2	0.002 (0.2)	0.01	Characteristic (0.7) Maximum Magnitude (0.3)	0.84
										90	7.4	0.6	0.009 (0.6)			
										50 W	7.7	0.2	0.015 (0.2)			
13	Jemez-San Ysidro fault	2029	152	Unsegmented	1	N	<15 ka	96	25	58 E	7.1	0.2	0.009 (0.2)	0.03	Characteristic (0.7) Maximum Magnitude (0.3)	0.84
										75 E	7.4	0.6	0.031 (0.6)			
										90	7.7	0.2	0.054 (0.2)			
14	Jornada Draw fault	2056	304	Unsegmented	1	N	<750 ka	65	25	45 E	7.0	0.2	0.018 (0.2)	0.06	Characteristic (0.7) Maximum Magnitude (0.3)	0.84
										60 E	7.3	0.6	0.06 (0.6)			
										75 E	7.6	0.2	0.1 (0.2)			
15	La Bajada fault	2032	197	Unsegmented	1	N	<1.6 Ma	48	25	55 W	6.8	0.2	0.079 (0.2)	0.09	Characteristic (0.7) Maximum Magnitude (0.3)	0.84
										70 W	7.1	0.6	0.095 (0.6)			
										90 W	7.4	0.2	0.11 (0.2)			



Table 4-2 cont.: PSHA Input Parameters

No.	Fault	Fault Number <sup>(1)</sup>	Distance from Site (km)	Rupture Model	Probability of Activity	Sense of Slip	Time Since Most Recent Deformation	Max Rupture Length (km)	Seismogenic Depth (km)	Dip	M <sub>max</sub> <sup>(2)</sup>	Weighting	Slip Rate (mm/yr)	Weighted Mean of Slip Rate	Recurrence Model	b-value
16	La Jencia fault	2109	195	Unsegmented	1	N	<15 ka	34	25	70 E	6.6	0.2	0.033 (0.2)	0.04	Characteristic (0.7) Maximum Magnitude (0.3)	0.84
										80 E	6.9	0.6	0.039 (0.6)			
										90 E	7.2	0.2	0.045 (0.2)			
17	Leupp faults	1017	239	Unsegmented	1	N	<750 ka	32	25	50 W	6.6	0.2	0.001 (0.2)	0.10	Characteristic (0.7) Maximum Magnitude (0.3)	0.84
										90	6.9	0.6	0.1 (0.6)			
										50 E	7.2	0.2	0.2 (0.2)			
18	Loma Pelada fault	2113	192	Unsegmented	1	N	<130 ka	44	25	60 E	6.8	0.2	0.001 (0.2)	0.10	Characteristic (0.7) Maximum Magnitude (0.3)	0.84
										70 E	7.1	0.6	0.1 (0.6)			
										85 E	7.4	0.2	0.2 (0.2)			
19	Manzano fault	2119	203	Unsegmented	1	N	<750 ka	54	25	35 W	7.0	0.2	0.001 (0.2)	0.10	Characteristic (0.7) Maximum Magnitude (0.3)	0.84
										50 W	7.3	0.6	0.1 (0.6)			
										65 W	7.6	0.2	0.2 (0.2)			
20	McCormick Ranch faults	2135	184	Unsegmented	1	N	<750 ka	13	25	50 E	6.2	0.2	0.004 (0.2)	0.01	Characteristic (0.7) Maximum Magnitude (0.3)	0.84
										90	6.5	0.6	0.011 (0.6)			
										50 W	6.8	0.2	0.017 (0.2)			
21	Nacimiento fault	2002a	148	Northern segment	1	N	<1.6 Ma	36	25	45 E	6.8	0.2	0.001 (0.2)	0.10	Characteristic (0.7) Maximum Magnitude (0.3)	0.84
										50 E	7.1	0.6	0.1 (0.6)			
										60 E	7.4	0.2	0.2 (0.2)			
		2002b	146	Southern segment	N	<750 ka	45	25	75 E	6.8	0.2	0.01 (0.2)	0.17	Characteristic (0.7) Maximum Magnitude (0.3)		
									80 E	7.1	0.6	0.2 (0.6)				
									90 E	7.4	0.2	0.23 (0.2)				
2002a,b	146	Unsegmented (0.2)	1	N	<750 ka	82	25	45 E	7.1	0.2	0.001 (0.2)	0.10	Characteristic (0.7) Maximum Magnitude (0.3)			
								65 E	7.4	0.6	0.1 (0.6)					
								90 E	7.7	0.2	0.2 (0.2)					
22	Nambe fault	2024	232	Unsegmented	1	N	<1.6 Ma	48	25	50 E	6.8	0.2	0.01 (0.2)	0.06	Characteristic (0.7) Maximum Magnitude (0.3)	0.84
										90	7.1	0.6	0.02 (0.6)			
										50 W	7.4	0.2	0.23 (0.2)			
23	Northern Sangre de Cristo fault	2321	319	Unsegmented	1	N	<15 ka	168	25	35 W	7.4	0.2	0.001 (0.2)	0.06	Characteristic (0.7) Maximum Magnitude (0.3)	0.84
										50 W	7.7	0.6	0.044 (0.6)			
										65 W	8.0	0.2	0.164 (0.2)			
24	Pajarito fault zone	2008	195	Unsegmented	1	N	<15 ka	49	25	35 E	6.9	0.2	0.033 (0.2)	0.10	Characteristic (0.7) Maximum Magnitude (0.3)	0.84
										50 E	7.2	0.6	0.1 (0.6)			
										65 E	7.5	0.2	0.167 (0.2)			
25	Picuris-Pecos fault (Class B)	2023	238	Unsegmented	1	N	<1.6 Ma	98	25	70 W	7.1	0.2	0.01 (0.2)	0.12	Characteristic (0.7) Maximum Magnitude (0.3)	0.84
										90	7.4	0.6	0.05 (0.6)			
										70 E	7.7	0.2	0.45 (0.2)			
26	Pojoaque fault zone	2010	221	Unsegmented	1	N	<1.6 Ma	48	25	60 E	6.8	0.2	0.01 (0.2)	0.06	Characteristic (0.7) Maximum Magnitude (0.3)	0.84
										90	7.1	0.6	0.02 (0.6)			
										60 W	7.4	0.2	0.23 (0.2)			
27	San Felipe fault zone	2030	164	Unsegmented	1	N	<1.6 Ma	89	25	60 E	7.1	0.2	0.035 (0.2)	0.04	Characteristic (0.7) Maximum Magnitude (0.3)	0.84
										90	7.4	0.6	0.043 (0.6)			
										64 W	7.7	0.2	0.05 (0.2)			
28	Sand Hill fault zone	2039	150	Unsegmented	1	N	<1.6 Ma	36	25	54 E	6.7	0.2	0.001 (0.2)	0.10	Characteristic (0.7) Maximum Magnitude (0.3)	0.84
										68 E	7.0	0.6	0.1 (0.6)			
										82 E	7.3	0.2	0.2 (0.2)			

Table 4-2 cont.: PSHA Input Parameters

No.	Fault	Fault Number <sup>(1)</sup>	Distance from Site (km)	Rupture Model	Probability of Activity	Sense of Slip	Time Since Most Recent Deformation	Max Rupture Length (km)	Seismogenic Depth (km)	Dip	M <sub>max</sub> <sup>(2)</sup>	Weighting	Slip Rate (mm/yr)	Weighted Mean of Slip Rate	Recurrence Model	b-value
29	San Andres Mountains fault	2053	311	Unsegmented	1	N	<130 ka	114	25	35 E	7.3	0.2	0.002 (0.2)	0.08	Characteristic (0.7) Maximum Magnitude (0.3)	0.84
										50 E	7.6	0.6	0.06 (0.6)			
										65 E	7.9	0.2	0.21 (0.2)			
30	Santa Fe fault	2123	153	Unsegmented	1	N	<1.6 Ma	30	25	45 E	6.6	0.2	0.001 (0.2)	0.05	Characteristic (0.7) Maximum Magnitude (0.3)	0.84
										60 E	6.9	0.6	0.008 (0.6)			
										80 E	7.2	0.2	0.2 (0.2)			
31	Socorro Canyon fault zone	2108	210	Unsegmented	1	N	<130 ka	49	25	36 E	6.8	0.2	0.03 (0.2)	0.22	Characteristic (0.7) Maximum Magnitude (0.3)	0.84
										63 E	7.1	0.6	0.15 (0.6)			
										90	7.4	0.2	0.6 (0.2)			
32	Southern Sangre de Cristo fault	2017	272	Unsegmented	1	N	<15 ka	99	25	60 W	7.5	0.6	0.12 (0.6)	0.12	Characteristic (0.7) Maximum Magnitude (0.3)	0.84
											7.8	0.2	0.23 (0.2)			
											7.0	0.2	0.02 (0.2)			
33	Tijeras-Cañoncito fault system	2033	195	Unsegmented	1	SS	<130 ka	79	25	90	7.3	0.6	0.09 (0.6)	0.20	Characteristic (0.7) Maximum Magnitude (0.3)	0.84
											7.6	0.2	0.72 (0.2)			
											6.1	0.2	0.001 (0.2)			
34	Unnamed fault of Bonita Canyon (Class B)	2144	88	Unsegmented	1	N	<1.6 Ma	9	25	50 W	6.1	0.2	0.001 (0.2)	0.10	Characteristic (0.7) Maximum Magnitude (0.3)	0.84
											6.4	0.6	0.1 (0.6)			
											6.7	0.2	0.2 (0.2)			
35	Unnamed faults along San Mateo Mountains	2131	233	Unsegmented	1	N	<750 ka	41	25	35 W	6.8	0.2	0.009 (0.2)	0.01	Characteristic (0.7) Maximum Magnitude (0.3)	0.84
											7.1	0.6	0.01 (0.6)			
											7.4	0.2	0.011 (0.2)			
36	Unnamed faults of El Malpais lava field (Class B)	2146	89	Unsegmented	1	N	<1.6 Ma	26	25	45 W	6.5	0.2	0.001 (0.2)	0.10	Characteristic (0.7) Maximum Magnitude (0.3)	0.84
											6.8	0.6	0.1 (0.6)			
											7.1	0.2	0.2 (0.2)			
37	Unnamed faults near Albuquerque Volcanoes	2049	162	Unsegmented	1	N	<750 ka	34	25	50 E	6.6	0.2	0.005 (0.2)	0.01	Characteristic (0.7) Maximum Magnitude (0.3)	0.84
											6.9	0.6	0.009 (0.6)			
											7.2	0.2	0.013 (0.2)			
38	Unnamed faults near Star Heights	2048	163	Unsegmented	1	N	<750 ka	18	25		6.4	0.2	0.001 (0.2)	0.100	Characteristic (0.7) Maximum Magnitude (0.3)	0.84
											6.7	0.6	0.1 (0.6)			
											7.0	0.2	0.2 (0.2)			
39	Unnamed faults on the Llano de Manzano	2117	203	Unsegmented	1	N	<750 ka	68	25	50 E	6.9	0.2	0.005 (0.2)	0.01	Characteristic (0.7) Maximum Magnitude (0.3)	0.84
											7.2	0.6	0.013 (0.6)			
											7.5	0.2	0.02 (0.2)			
40	Vernon fault zone	1016	176	Unsegmented	1	N/SS	<750 ka	57	25	35 NE	7.0	0.2	0.001 (0.2)	0.10	Characteristic (0.7) Maximum Magnitude (0.3)	0.84
											7.3	0.6	0.1 (0.6)			
											7.6	0.2	0.2 (0.2)			
41	West Joyita fault zone	2110	212	Unsegmented	1	N	<1.6 Ma	48	25	41 W	6.8	0.2	0.001 (0.2)	0.10	Characteristic (0.7) Maximum Magnitude (0.3)	0.84
											7.1	0.6	0.1 (0.6)			
											7.4	0.2	0.2 (0.2)			
42	Zia fault	2046	157	Unsegmented	1	N	<15 ka	32	25	35 E	6.7	0.2	0.055 (0.2)	0.08	Characteristic (0.7) Maximum Magnitude (0.3)	0.84
											7.0	0.6	0.078 (0.6)			
											7.3	0.2	0.1 (0.2)			
											Activity Rates	0.34	Exponential (1.0)	0.79(0.2)		
												0.19		0.84(0.6)		
											a-value	3.49		0.89(0.2)		

Notes:

1. Following number scheme used by USGS.
2. Maximum magnitudes estimated using the empirical relation of Wells and Coppersmith (1994) for Normal Faults based on rupture area.

**Table 5-1: GMPEs used in the PSHA**

GMPE	Weight
Abrahamson et al. (2014)	0.25
Boore et al. (2014)	0.25
Campbell and Bozorgnia (2014)	0.25
Chiou and Youngs (2014)	0.25

**Table 6-1: PSHA Input Parameters**

Input Parameter	Value		
$V_{s30}$ ft/s (m/s)	902 ft/s (275 m/s)	1,378 ft/s (420 m/s)	1,857 ft/s (566 m/s)
$Z_{1.0}$ (km)	0.472 km	0.337 km	0.166 km
$Z_{2.5}$ (km)	1.941 km	1.196 km	0.850 km

**Table 6-2: PSHA Results**

Return Period	$V_{s30}$ (ft/s)	$V_{s30}$ (m/s)	Mean PGA (g)
10,000	902	275	0.30
	1,348	420	0.28
	1,857	566	0.25

**Table 7-1: Deterministic Inputs and GMPEs**

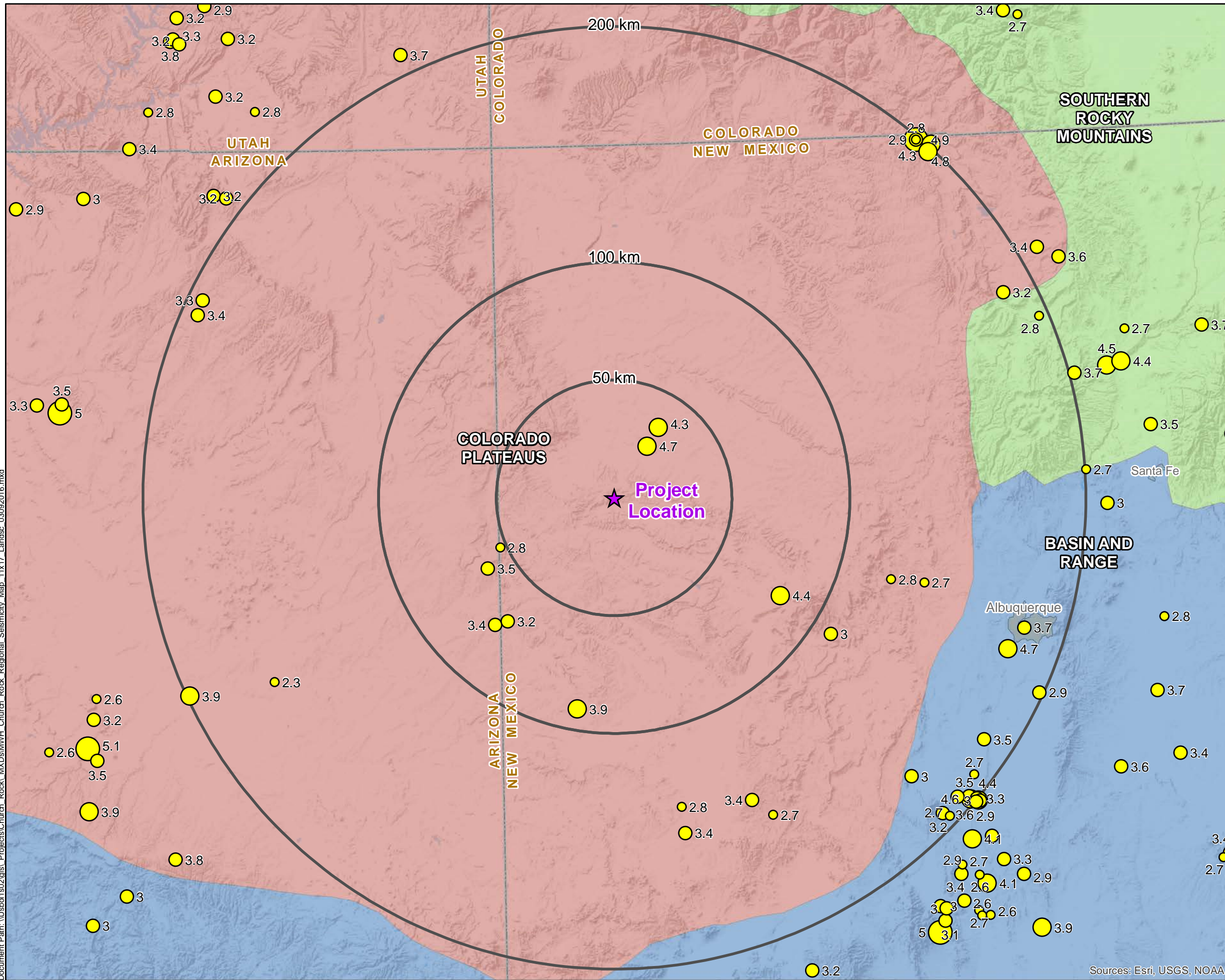
Deterministic Input Parameter	Intrabasin Faults of the Llano Albuquerque	Nacimiento Fault	San Felipe Fault	Jemez- San Ysidro Fault
M <sub>w</sub>	7.4	7.4	7.4	7.4
R <sub>RUP</sub> (km)	158	124	164	152
R <sub>JB</sub> (km)	158	124	164	152
R <sub>x</sub> (km)	158	124	164	152
V <sub>s30</sub> (m/s)	275	275	275	275
Hanging Wall	NO	NO	NO	NO
Fault Mechanism	Normal	Normal	Normal	Normal
Dip (deg)	50	50	50	75
Z <sub>TOR</sub> (km)	0	0	0	0
Z <sub>HYP</sub> (km)	10.3 (Default)	10.3	10.3 (Default)	10.3 (Default)
Z <sub>1.0</sub> (km)	0.47 (Default)	0.47	0.47 (Default)	0.47 (Default)
Z <sub>2.5</sub> (km)	1.94 (Default)	1.94	1.94 (Default)	1.94 (Default)
W (km)	33	33	33	33
V <sub>s30</sub> Flag	Estimated	Estimated	Estimated	Estimated
Region	Global	Global	Global	Global
GMPE	ASK14, BSSA14, CB14, and CY14	ASK14, BSSA14, CB14, and CY14	ASK14, BSSA14, CB14, and CY14	ASK14, BSSA14, CB14, and CY14

**Table 7-2: Deterministic PGA Values**

Seismic Source	Magnitude	R <sub>RUP</sub> Distance (km)	PGA (g)	
			50 <sup>th</sup> Percentile (Median)	84 <sup>th</sup> Percentile (Median+1σ)
Intrabasin Faults of the Llano Albuquerque	7.4	158	0.03	0.05
Nacimiento Fault	7.4	124	0.04	0.07
San Felipe Fault	7.4	164	0.02	0.04
Jemez- San Ysidro Fault	7.4	152	0.03	0.05

## FIGURES

Document Path: \\usbof\is02\gis\Projects\Church\_Rock\MXD\MWH\_Church\_Rock\_Regional\_Seismicity\_Map\_11x17\_Landsc\_03092016.mxd



# LEGEND

★ Project Location

□ Project Buffer

### Magnitude

- 2.3 - 2.9
- 3.0 - 3.9
- 4.0 - 4.9
- 5.0 - 5.1

### Physiographic Province

- Basin and Range
- Colorado Plateaus
- Southern Rocky Mountains



0 15 30 60 Miles

0 25 50 100 km

TITLE: Regional Seismicity

PROJECT: NECR Seismic Hazard Assessment

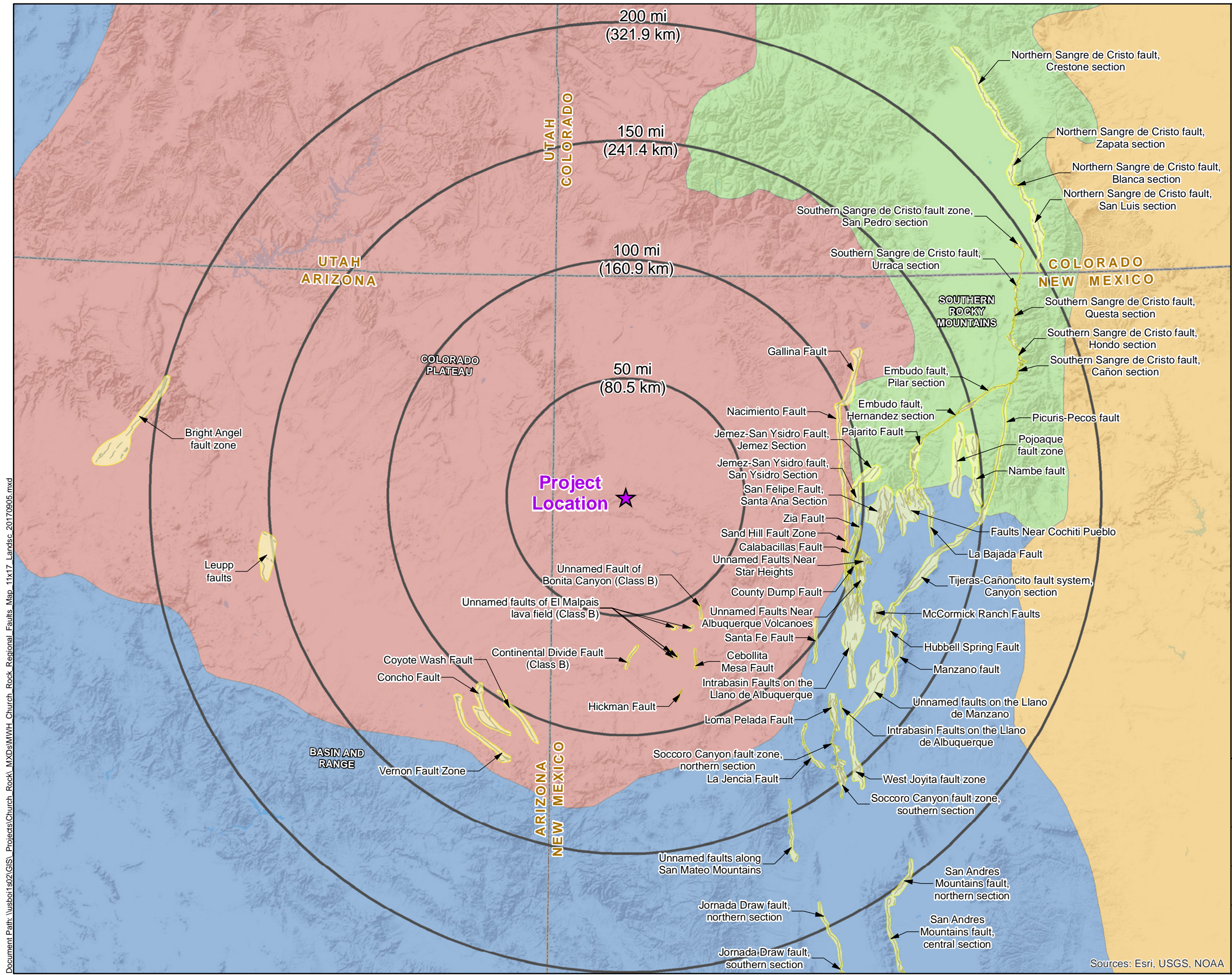
REFERENCE(S):  
Coordinate System:  
NAD 1983 UTM Zone 12N  
Units: Meter



OCTOBER 2017

FIGURE: 1-1

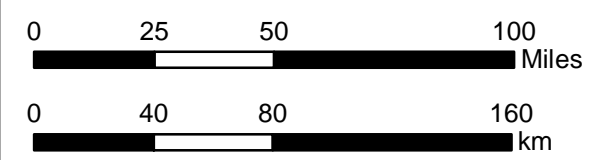
Sources: Esri, USGS, NOAA



# LEGEND

- Project Location
- Fault
- Fault Area (Delineated for Presentation Purposes Only)

- Physiographic Province**
- Basin and Range
  - Colorado Plateau
  - GREAT PLAINS
  - Southern Rocky Mountains



TITLE:  
**Regional Faults**

PROJECT:  
**NECR Seismic Hazard Assessment**

REFERENCE(S):  
Coordinate System:  
NAD 1983 HARN StatePlane New Mexico West FIPS 3003 Feet  
Units: Foot US

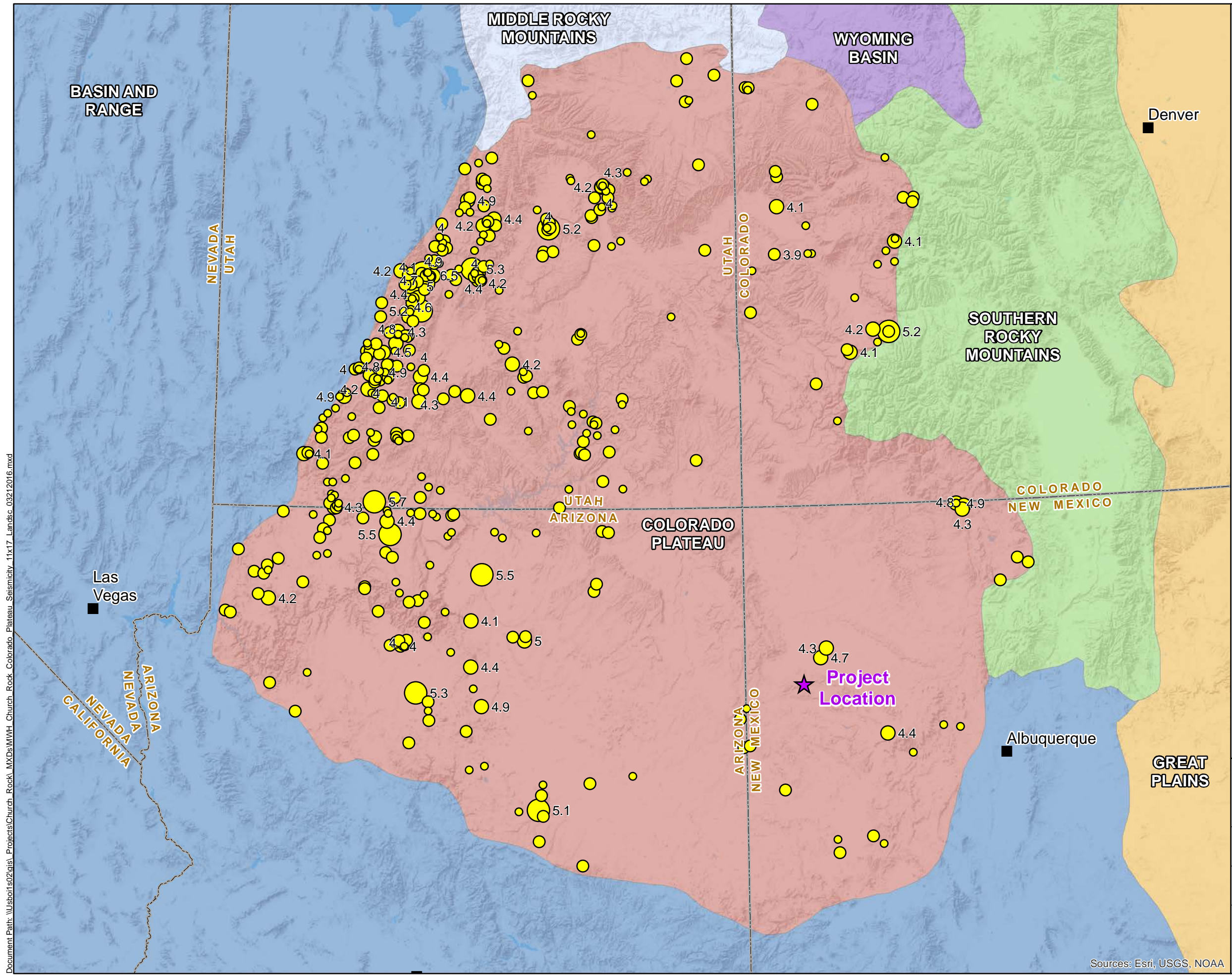
OCTOBER 2017

FIGURE:  
**2-1**

MWH now part of Stantec

Document Path: \\usba11s02\GIS\Projects\Church\_Rock\MXD\MWH\_Church\_Rock\_Regional\_Faults\_Map\_11x17\_Landsc\_20170905.mxd

Sources: Esri, USGS, NOAA



# LEGEND

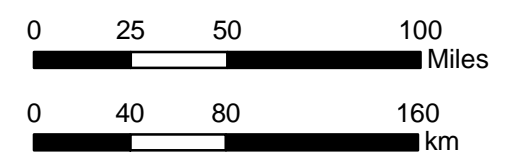
- ★ Project Location
- City

## Magnitude

- 2.3 - 3.0
- 3.1 - 4.0
- 4.1 - 5.0
- 5.1 - 6.0
- 6.1 - 6.5

## Physiographic Province

- Basin and Range
- Colorado Plateau
- Great Plains
- Middle Rocky Mountains
- Southern Rocky Mountains
- Wyoming Basin



TITLE:  
**Seismicity of the Colorado Plateau**

PROJECT:  
**NECR Seismic Hazard Assessment**

REFERENCE(S):  
Coordinate System:  
NAD 1983 UTM Zone 12N  
Units: Meter

OCTOBER 2017

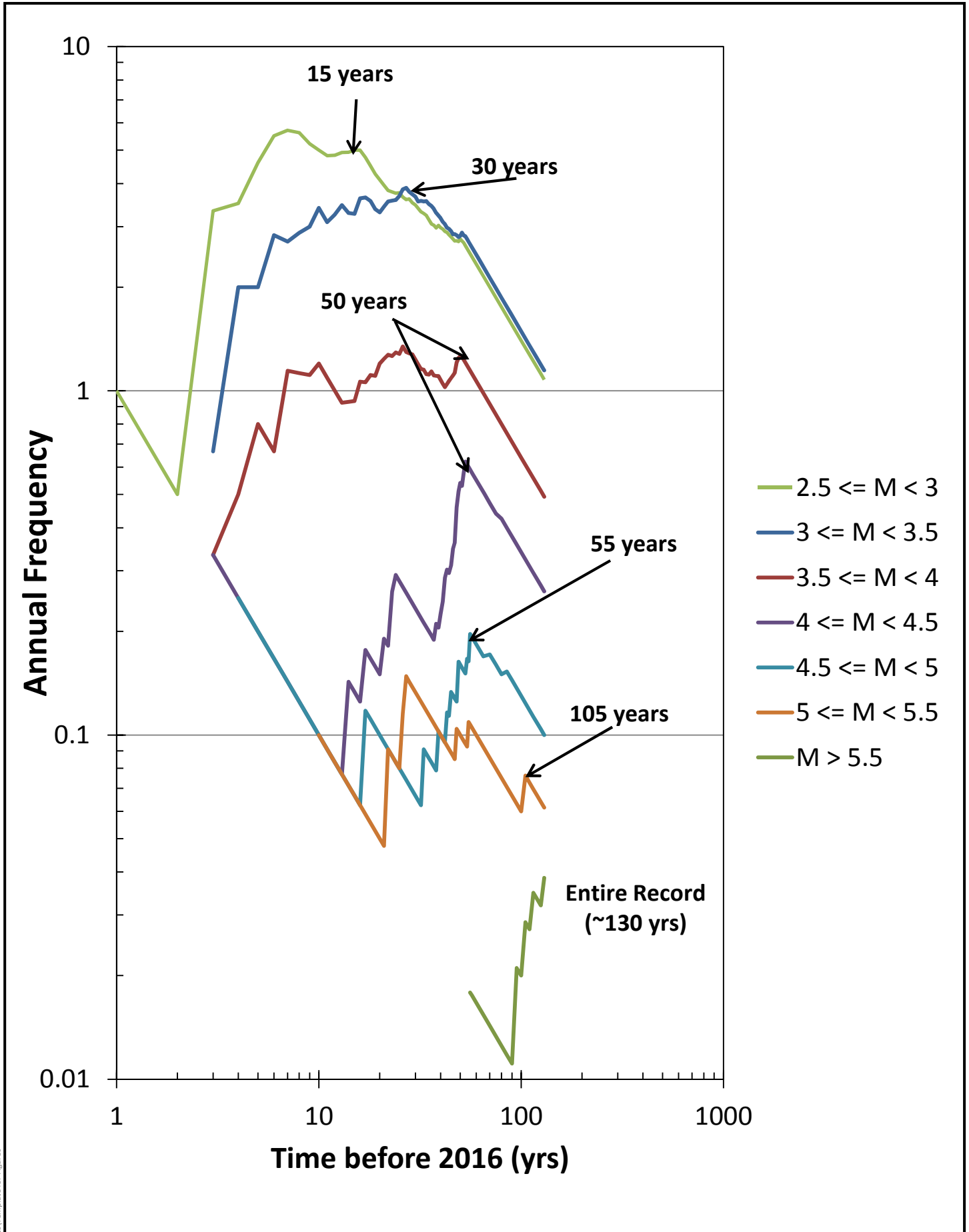
FIGURE:  
**3-1**

MWH Stantec



Document Path: \\usboif02\gis\Projects\Church\_Rock\MXD\MWH\_Church\_Rock\_Colorado Plateau\_Seismicity\_11x17\_Landsc\_03212016.mxd

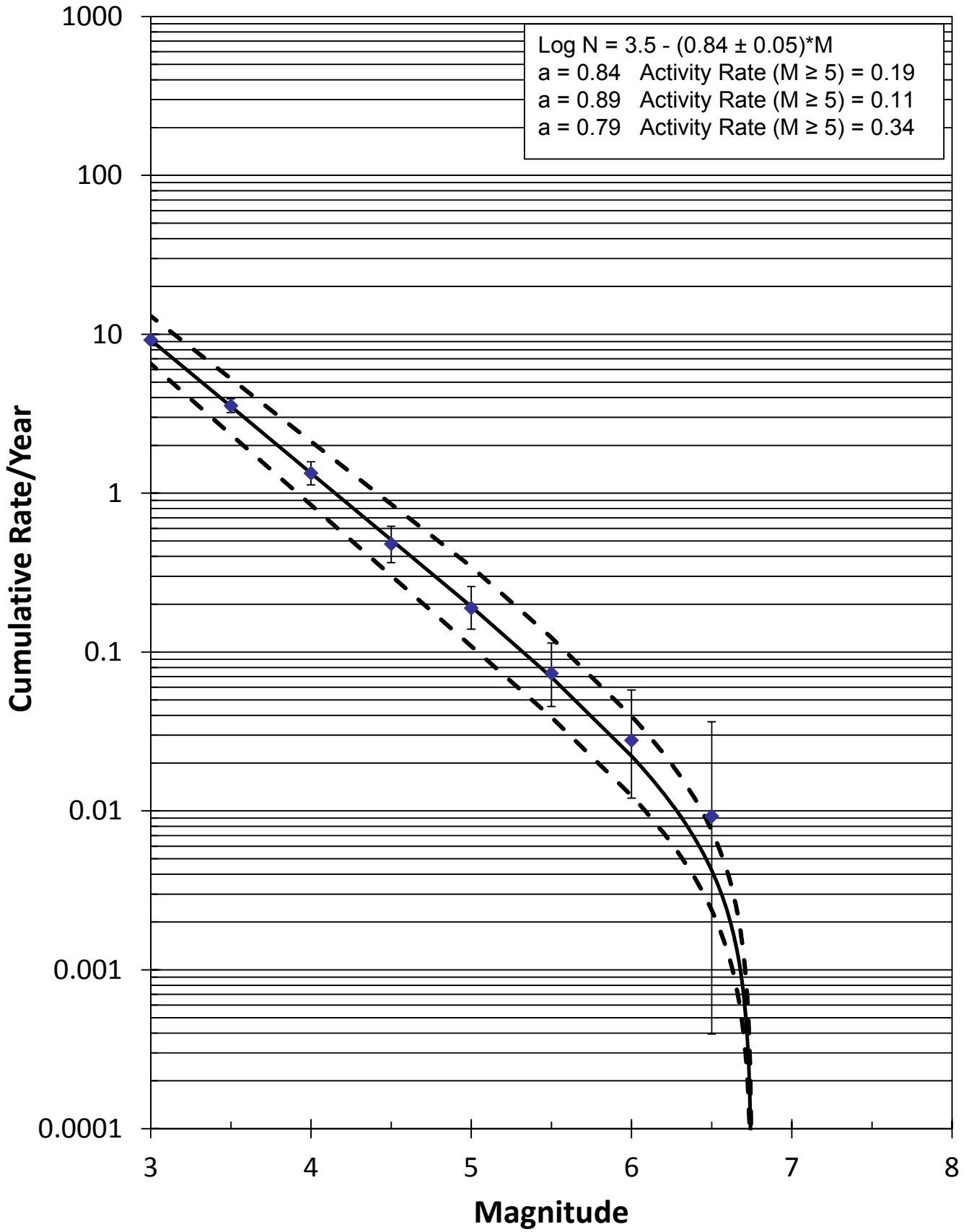
Sources: Esri, USGS, NOAA







P:\Administrative\MWH Reports\Template\Figures

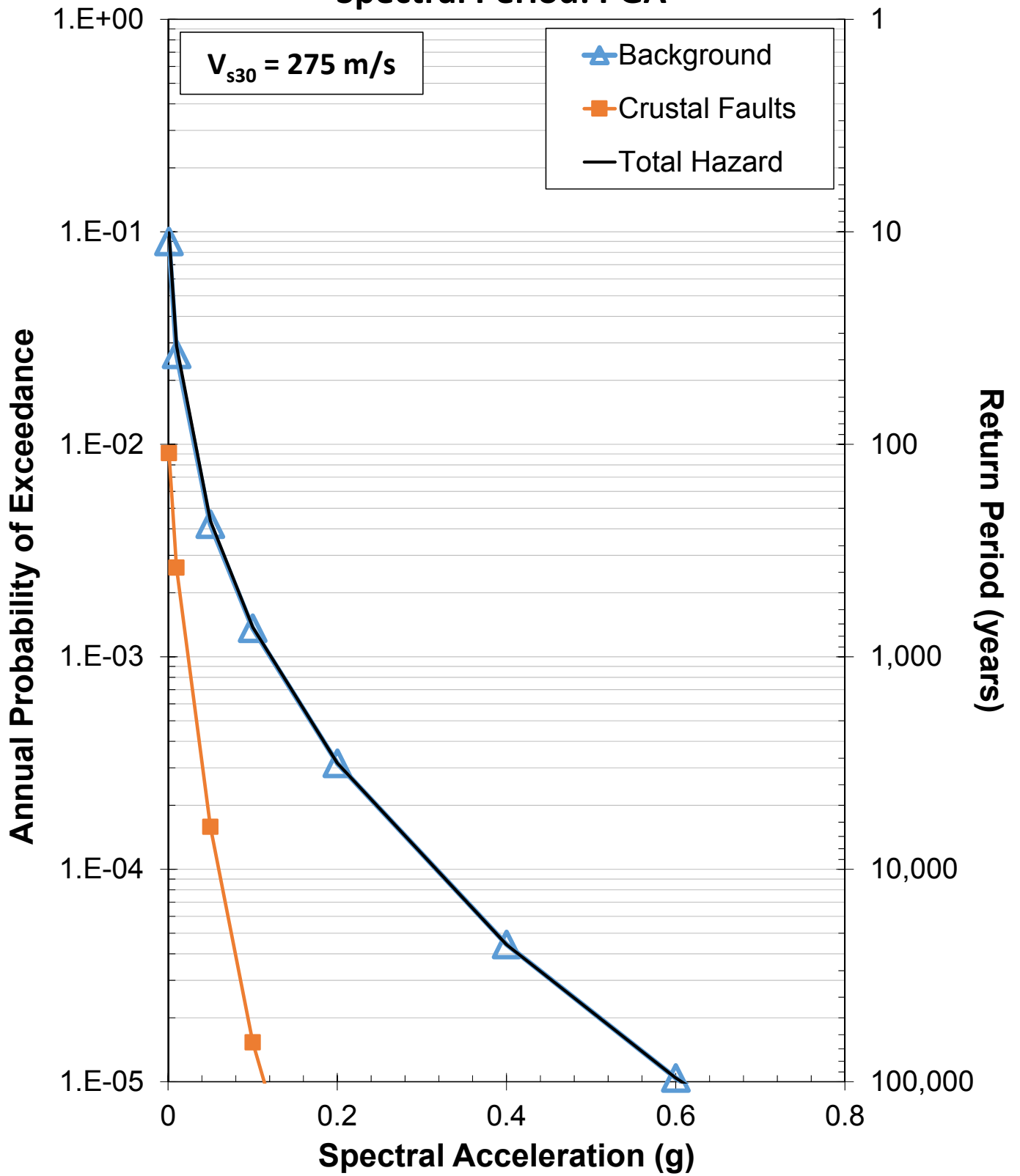
		PROJECT NECR SEISMIC HAZARD ASSESSMENT	 MWH <small>now part of</small>  Stantec	
		TITLE CATALOG COMPLETENESS PLOTS	DATE OCT 2017	FIGURE 3-2
			FILENAME	





P:\Administrative\MWH Reports\Templates\Template for Figures

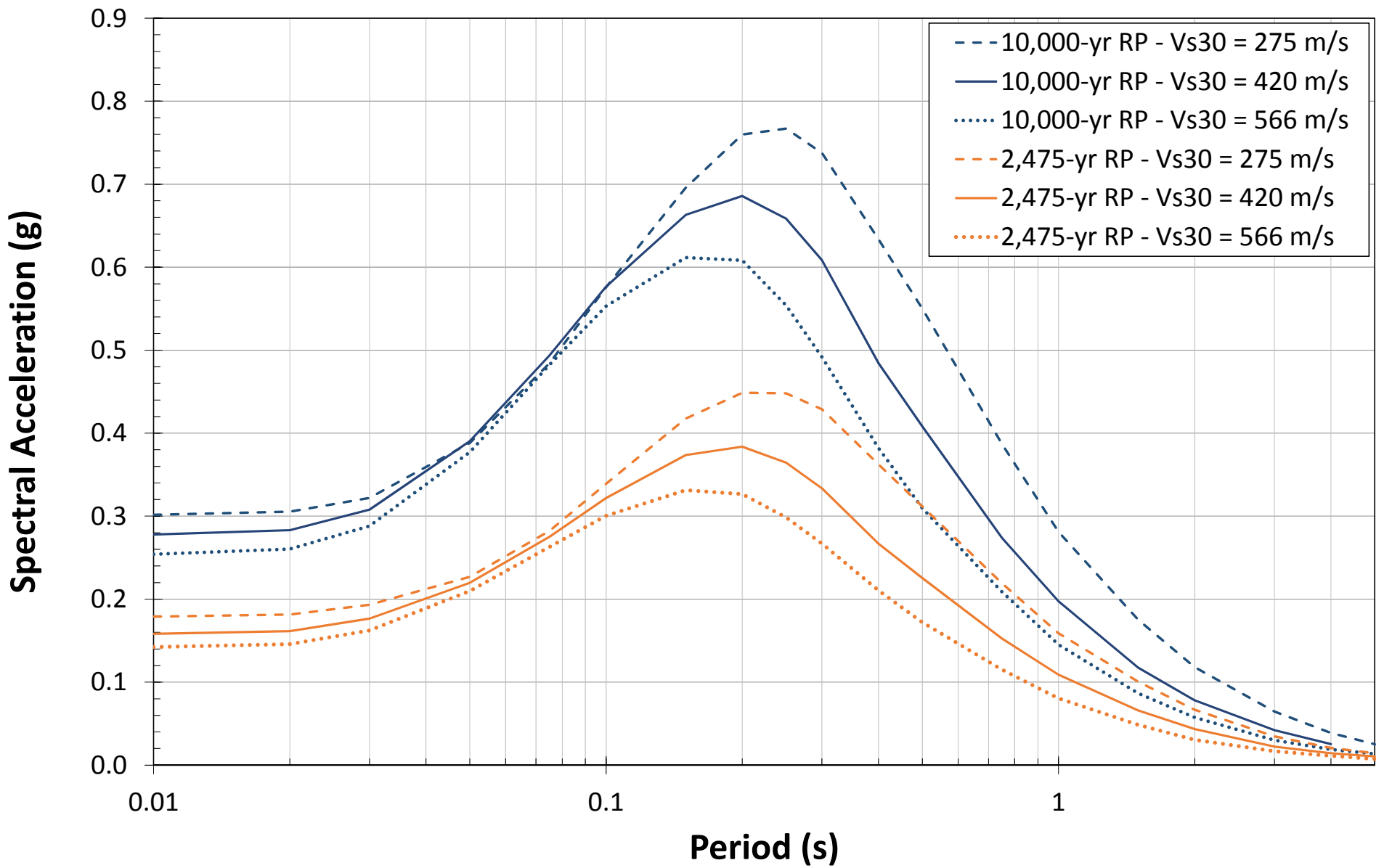
PROJECT	NECR SEISMIC HAZARD ASSESSMENT		 MWH <small>now part of</small>  Stantec
	TITLE	GUTENBERG-RICHTER RELATIONSHIP COLORADO PLATEAU	
DATE	OCT 2017	FIGURE	4-1
FILENAME			

# Spectral Period: PGA



P:\Administrative\MWH Reports\Template for Figures

		PROJECT NECR SEISMIC HAZARD ASSESSMENT	 	
		TITLE PEAK GROUND ACCELERATION SEISMIC SOURCE CONTRIBUTION	DATE OCT 2017	FIGURE 6-1
			FILENAME	



PROJECT  
NECR SEISMIC HAZARD ASSESSMENT

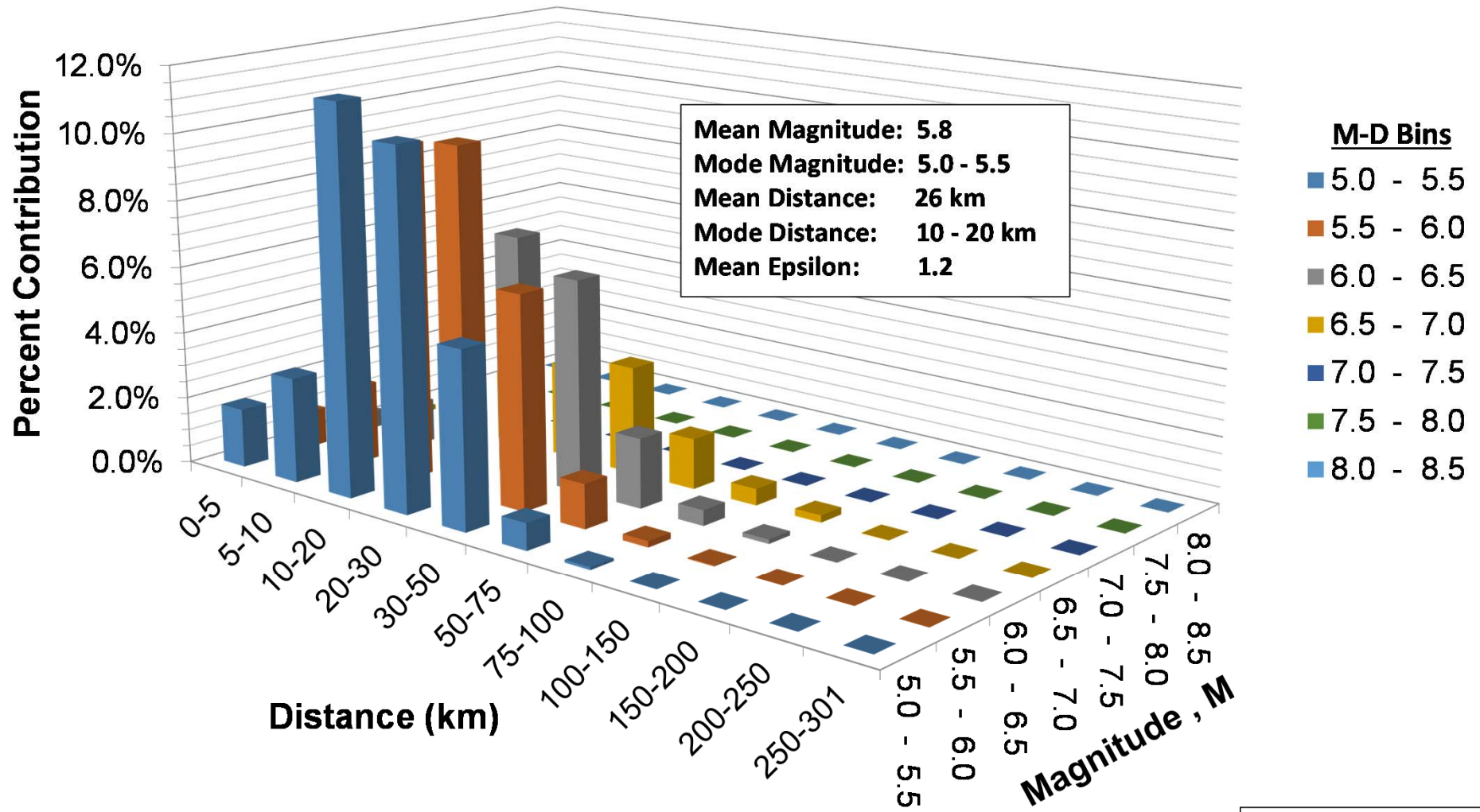


TITLE  
UNIFORM HAZARD SPECTRA  
COMPARISON OF Vs30

DATE  
OCT 2017



FIGURE 6-2

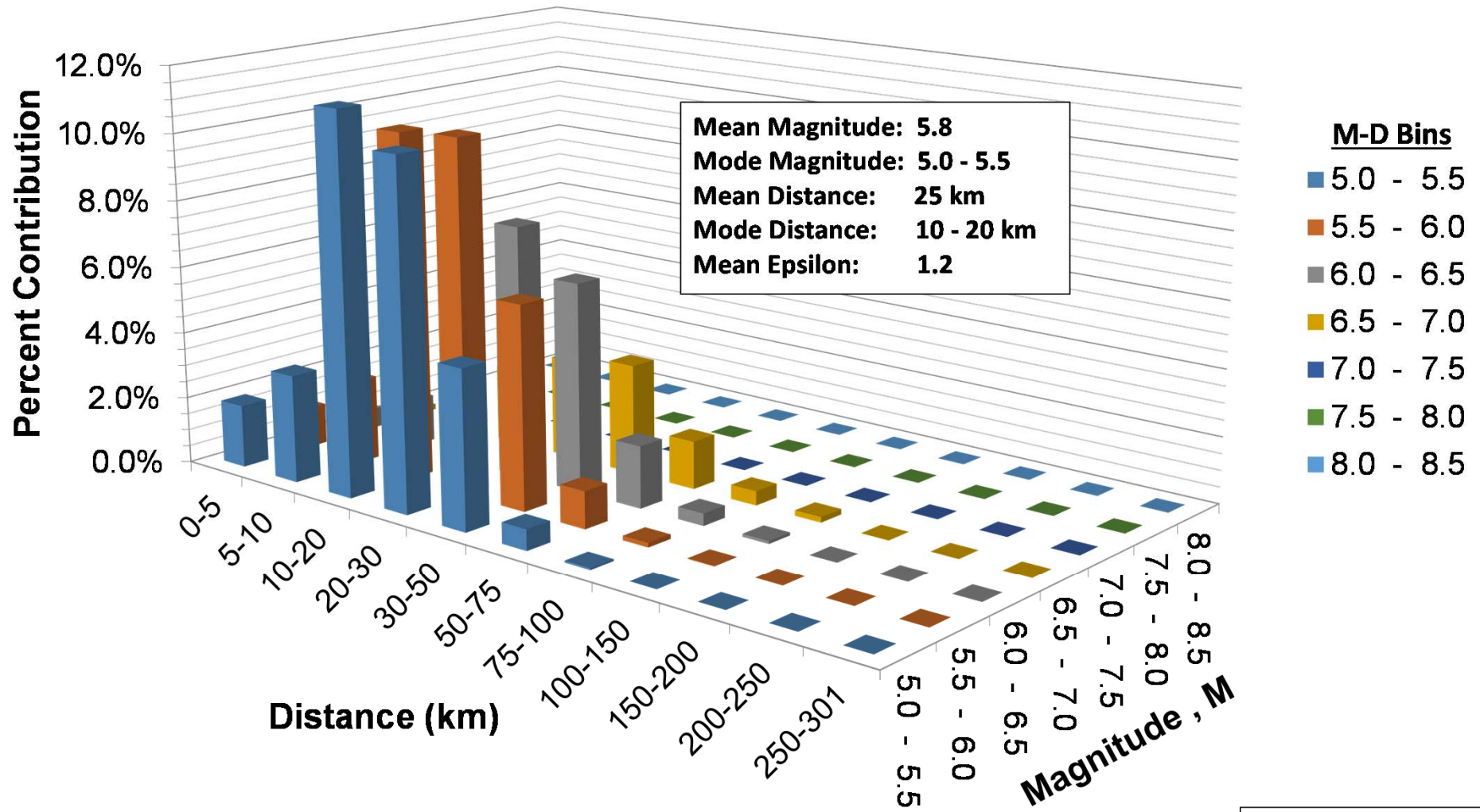
FILENAME



10,000-yr Return Period, PGA



$V_{s30} = 275 \text{ m/s}$

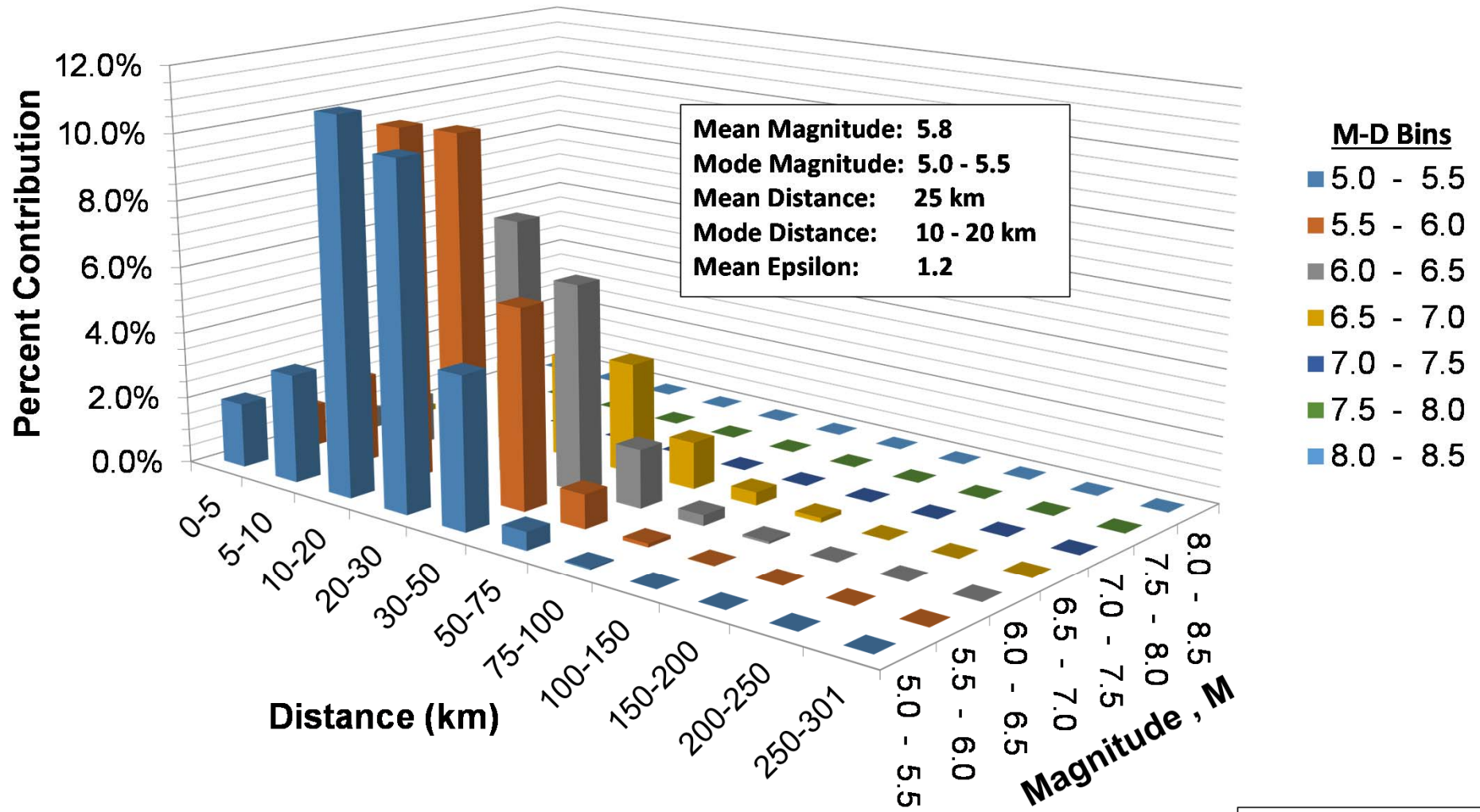
PROJECT	NECR SEISMIC HAZARD ASSESSMENT		 
TITLE	DEAGGREGATION OF PGA 10,000-YEAR RETURN PERIOD (Vs30 = 275 m/s)		
DATE	OCT 2017	FIGURE 6-3	FILENAME



10,000-yr Return Period, PGA



$V_{s30} = 420 \text{ m/s}$

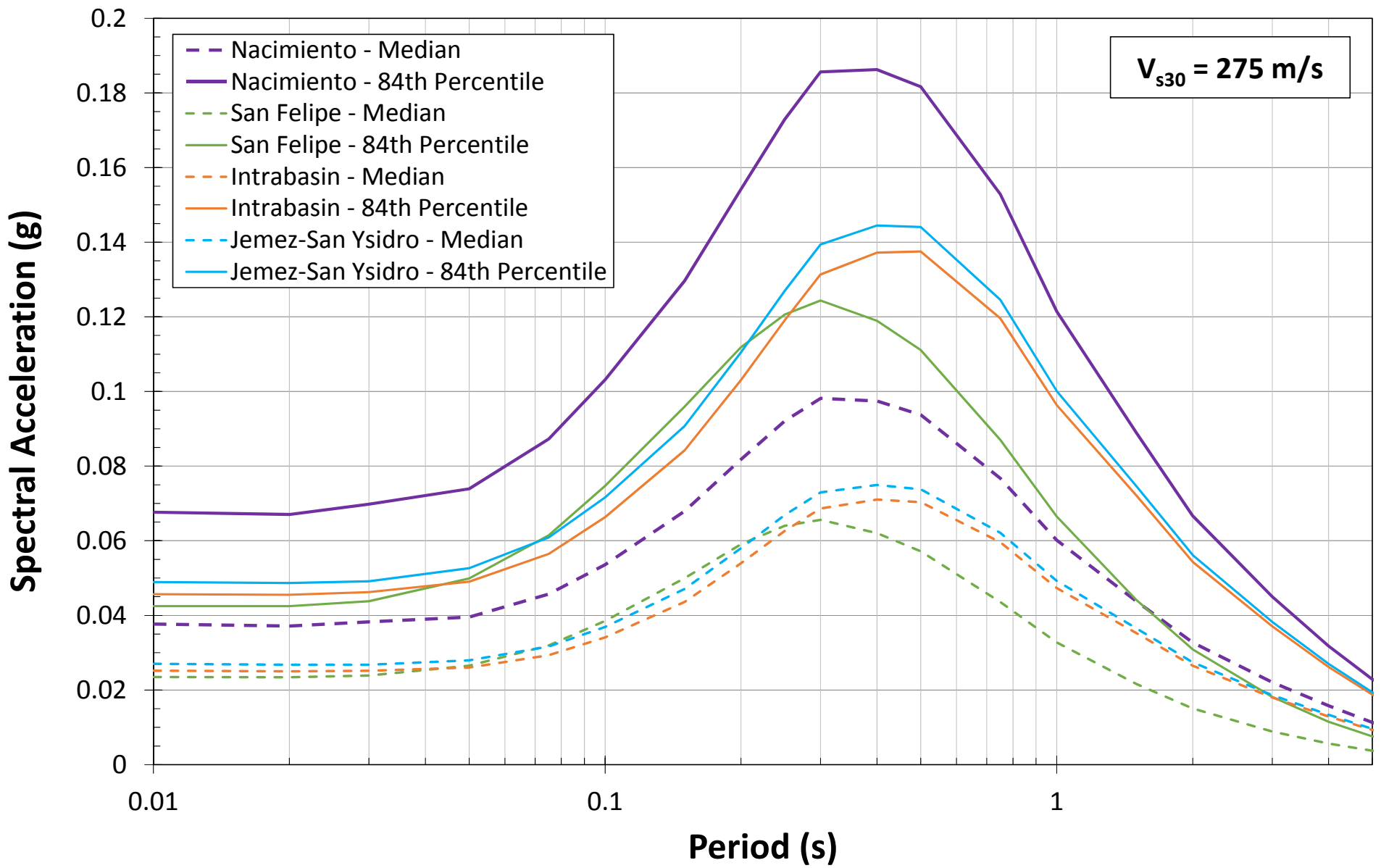
PROJECT	NECR SEISMIC HAZARD ASSESSMENT		 
TITLE	DEAGGREGATION OF PGA 10,000-YEAR RETURN PERIOD ( $V_{s30} = 420 \text{ m/s}$ )		
DATE	OCT 2017	FIGURE 6-4	FILENAME



10,000-yr Return Period, PGA

$V_{s30} = 566 \text{ m/s}$

PROJECT	NECR SEISMIC HAZARD ASSESSMENT		 
TITLE	DEAGGREGATION OF PGA 10,000-YEAR RETURN PERIOD ( $V_{s30} = 566 \text{ m/s}$ )		
DATE	OCT 2017	FIGURE 6-5	FILENAME



PROJECT  
NECR SEISMIC HAZARD ASSESSMENT

TITLE  
DETERMINISTIC RESPONSE SPECTRA –  
MEDIAN & 84<sup>th</sup> PERCENTILE  
FOR  $V_{s30} = 275 \text{ m/s}$

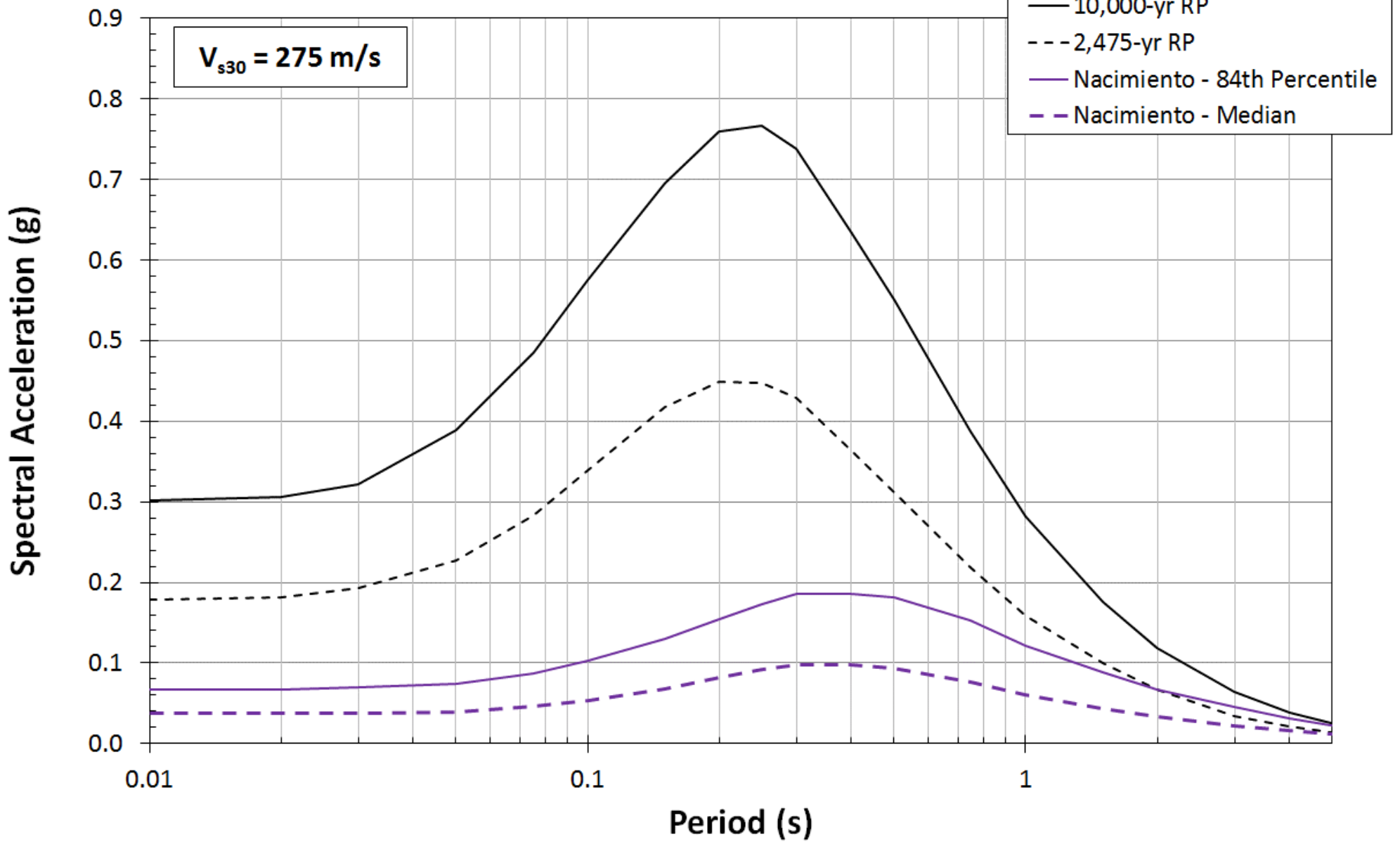
MWH now part of Stantec

DATE  
OCT 2017

FIGURE 7-1

FILENAME





PROJECT  
NECR SEISMIC HAZARD ASSESSMENT

TITLE  
COMPARISON OF DETERMINISTIC  
RESPONSE SPECTRA & UHS  
FOR  $V_{s30} = 275 \text{ m/s}$

MWH now part of Stantec

DATE  
OCT 2017

FIGURE 8-1

FILENAME